

Prediction of Subjective Discomfort Caused by Optical Distortion in VR Headsets  
During Head Movements Triggering Vestibulo-Ocular Reflex on Static VR Scenes

By

CHAN, Tsz Tai

A Thesis Submitted to  
The Hong Kong University of Science and Technology  
in Partial Fulfillment of the Requirements for  
the Degree of Master of Philosophy  
in Industrial Engineering and Decision Analytics

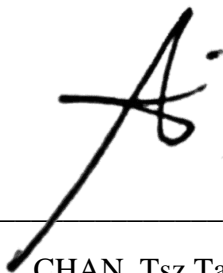
January 2021, Hong Kong

### **Authorization**

I hereby declare that I am the sole author of the thesis.

I authorize the Hong Kong University of Science and Technology to lend this thesis to other institutions or individuals for the purpose of scholarly research.

I further authorize the Hong Kong University of Science and Technology to reproduce the thesis by photocopying or by other means, in total or in part, at the request of other institutions or individuals for the purpose of scholarly research.

A handwritten signature in black ink, appearing to be 'Tsz Tai Chan', is written over a horizontal line. The signature is stylized with a large 'A' and a dot.

CHAN, Tsz Tai

19 January 2021

Prediction of Subjective Discomfort Caused by Optical Distortion in VR Headsets  
During Head Movements Triggering Vestibulo-Ocular Reflex on Static VR Scenes

By

CHAN, Tsz Tai

This is to certify that I have examined the above MPhil thesis  
and have found that it is complete and satisfactory in all respects,  
and that any and all revisions required by  
the thesis examination committee have been made.

---

Professor Richard H.Y. SO (Supervisor)

---

Professor Guillermo GALLEGO (Head of the Department)

Department of Industrial Engineering and Decision Analytics

19 January 2021

## **Acknowledgements**

First, I would like to express my very great appreciation to my supervisor, Professor Richard Hau Yue SO for giving me years of guidance to gradually improve my thinking process especially in identifying and solving problems, as well as my communication skills. Your profound knowledge helped me to better understand the research questions and your encouragement always made me feel spirited to continue my work and study.

High tribute shall be paid to my thesis examination committee members, Prof. Ravindra S. GOONETILLEKE and Prof. Ning CAI. Thank you for offering your expertise to provide valuable comments for me to revise my works.

I'm also deeply indebted to all the tutors and teachers from the courses that I took during my study in HKUST for their patient and careful help.

I would also like to thank my groupmates who have helped me to analysis problems and provided their unique suggestions.

Special thanks go to Yixuan WANG and Jerry JIA for the cooperation on the research project and the invaluable advice.

I shall also extend my gratitude to all subjects for giving patience and efforts when participated in my experiments.

Last but not least, I would like to thank my beloved family and all my friends for their encouragement and support during difficult times.

## TABLE OF CONTENTS

Title Page .....	i
Authorization Page.....	ii
Signature Page .....	iii
Acknowledgements .....	iv
List of Figures .....	viii
Abstract .....	ix
CHAPTER 1. INTRODUCTION .....	1
Summary .....	1
1.1 Introduction and research scope.....	1
1.2 Definition of terms .....	1
1.3 Background of the problem.....	2
1.4 Overview of the study .....	3
1.4.1 Experimental work .....	3
1.4.2 Predictive model development.....	4
CHAPTER 2. LITERATURE REVIEW .....	5
Summary .....	5
2.1 Visually induced motion sickness (VIMS) .....	5
2.2 Visual discomfort during VOR .....	6
2.3 Vection and VIMS .....	8
2.4 Visual motion sensitivity across field of view (FOV) .....	8
CHAPTER 3. EXPERIMENTS .....	10
Summary .....	10
3.1 Introduction.....	10
3.2 Pilot study 1 - Visual sensitivity during VOR .....	10
3.2.1 Objectives .....	10
3.2.2 Hypothesis.....	11
3.2.3 Method .....	11
3.2.4 Results.....	13
3.2.5 Analysis and Discussion .....	14
3.3 Pilot study 2 – Exploration of dynamic distortion .....	15
3.3.1 Objectives .....	15

3.3.2 Hypothesis.....	15
3.3.3 Method .....	15
3.3.4 Results.....	18
3.3.5 Discussion .....	19
3.4 Experiment 3 – Perceptual effect of dynamic distortion.....	20
3.4.1 Objectives .....	20
3.4.2 Hypothesis.....	21
3.4.3 Method .....	21
3.4.4 Results.....	23
3.4.5 Discussion .....	24
3.5 Experiment 4 – Validation of experiment question .....	24
3.5.1 Objectives .....	24
3.5.2 Hypothesis.....	25
3.5.3 Method .....	25
3.5.4 Result .....	26
3.5.5 Discussion .....	27
CHAPTER 4. PREDICTIVE MODEL.....	28
Summary .....	28
4.1 Introduction.....	28
4.2 Model development .....	28
4.2.1 Quantification of dynamic lens distortions .....	28
4.2.2 Applying weightings to distortions according to eccentricities .....	29
4.2.3 Smoothing to filter out large local distortion vector .....	30
4.2.4 Quantifying the spatial-temporal interactions between VOR head movements and the distortions in terms of 6 features.....	31
4.2.5 Modeling subjective discomfort as functions of the featured distortion .....	34
4.3 Model evaluation .....	35
4.4 Generalizing model.....	37
4.4.1 Selection of subjective rating scale.....	37
4.4.2 Selection of test cases to predict lens score .....	38
CHAPTER 5. DISCUSSION.....	40
5.1 Lens intrinsic performance.....	40
5.2 SSQ symptoms corresponding to discomfort score .....	41

5.3 Prediction on new lenses or cases with fixation not on x-axis (head tilting) .....	42
5.4 Estimating the scale at 90 <sup>th</sup> percentile of population for discomfort score .....	42
CHAPTER 6. CONCLUSIONS, LIMITATIONS AND FUTURE WORKS .....	44
6.1 Conclusions.....	44
6.2 Limitations and future works .....	45
6.2.1 Limitation.....	45
6.2.2 Future work .....	45
Bibliography and References .....	46
Appendix A. Set of localized distortion conditions in pilot study 1 .....	49
Appendix B. Observations on testing conditions in pilot study 2 and experiments 3 & 4 .....	50

## List of Figures

Figure 1. Two theories on VIMS .....	6
Figure 2. Hypothetical root cause of motion sickness in VR during VOR-type head motion...	8
Figure 3. Localized distortion (2D Gaussian-shape distortion). ....	12
Figure 4. Example of pilot study 1 procedure.....	13
Figure 5. Thresholds of localized distortions estimated at four sites .....	14
Figure 6. Visual scene used in pilot study 2 and experiment 3 and 4 .....	16
Figure 7. Dynamic distortion conditions used in pilot study 2 .....	16
Figure 8. Discomfort scale .....	17
Figure 9. Distortion scale .....	17
Figure 10. Mean of discomfort Scores in pilot study 2.....	19
Figure 11. The relationship between sum of magnitude and the scores rated for discomfort .	20
Figure 12. Lens-based conditions applied on participants in experiment 3 .....	22
Figure 13. Head motion control and controlled head motion .....	23
Figure 14. Mean of discomfort Scores of different lenses, modes and control intensity .....	24
Figure 15. Scores on A-0.5x (Left) and A-2x (Right) before and during 20-minute exposure	26
Figure 16. Scores of A-0.5x and A-2x between predicted and after the 20-min exposure .....	27
Figure 17. Visual scene, uncompensated and compensated distortion map .....	29
Figure 18. Justification over the FOV by elliptical weighting function .....	30
Figure 19. A distortion map before and after smoothing .....	31
Figure 20. Reprojecting a visual distortion map .....	32
Figure 21. Determination of probability width to filter valid distortion vectors .....	33
Figure 22. Determination of features' magnitude.....	34
Figure 23. Lens score calculation and selected features .....	35
Figure 24. Subject reported score against predicted score from model .....	36
Figure 25. Comparison between model prediction and subject reported rcores .....	37
Figure 26. Subjective rating scales and corresponding percentile estimation .....	38
Figure 27. Weighting Selections to comprise an overall lens performance score .....	39
Figure 28. Discomfort evaluation on lens intrinsic conditions .....	40
Figure 29. SSQ symptoms reported after 20-min exposure .....	41
Figure 30. Predicted distortion scores for lenses with fixation not on x-axis (head tilt) .....	42
Figure 31. Comparison between subject scale and MSSQ .....	43



# Prediction of Subjective Discomfort Caused by Optical Distortion in VR Headsets During Head Movements Triggering Vestibulo-Ocular Reflex on Static VR Scenes

By CHAN, Tsz Tai

Department of Industrial Engineering and Decision Analytics

The Hong Kong University of Science and Technology

## Abstract

Visual discomfort has been a major barrier to the popularization of Virtual Reality (VR) systems. There have been many studies on visual discomfort provoked by vection-inducing VR stimuli or mismatches between accommodations and binocular convergence during VR simulation. However, visual discomfort due to distorted images induced by optical aberration of lens inside VR headsets has received little attention. During head rotations, eye fixations are stabilized by vestibulo-ocular reflex (VOR) so that the projected image of an object remains stabilize on the retina. In VR simulations, because of inevitable imperfections in correction for lens optical aberration, visual distortions will occur during head motions when foveal view is stabilized by VOR. Little is known on how these distortions can affect human experience with different types and levels of lens aberration. The present work investigated the subjective discomfort induced by the dynamic distortion during active horizontal head rotation with a fixed gaze stabilized by VOR. Three experiments have been conducted, in which participants were instructed to rate their perceived visual discomfort in terms of disorientation and dizziness with different types and levels of dynamic distortion in a controlled VR scene. Higher subjective visual discomfort ratings were reported with increasing visual distortion even when the distortion was small. Significant effects of lens types on visual discomfort have been found. In addition to empirical investigation, an analytical model has been developed to predict the severity of such discomfort. The model can be a useful tool for VR headset industry because it takes in lens design parameters and predicts the associated visual discomfort. Results have been well received by the industry and is being deployed.

## **CHAPTER 1. INTRODUCTION**

### **Summary**

In this chapter, the motivation and scope of the research problem will be introduced. Some definition of terms used throughout the study will be explained to help understanding the work, then background of the problem and a brief overview of the study will be given.

### **1.1 Introduction and research scope**

Virtual reality (VR) headset is one of the most common form to simulate VR nowadays. To simulate a realistic visual environment, images with depth cues are rendered and displayed for both eyes in a VR headset. Besides, motion tracking system is usually applied to adjust visual input following user's movement. While the display is placed within a few inches in front of eyes, where it is difficult for human to focus on, lens is usually used to project the image to a further distance. Ideally, the combination of lens and display can reproduce the correct light rays entering the eye, given the optical system of the eye and the looking direction are determined. However, eye tracking technology is not yet mature enough that it is common for nowadays VR headsets to assume a fixed eye location and looking direction. Deviations from this assumption inevitably lead to distortion of the displayed images, and thus can provoke undesired experience. The distortion when the eyes are static is usually subtle and may not be noticeable, while when a viewer is turning head to one side and keeping eye gaze stabilized with VOR (the eyes are moving opposite to the head turns), the distortion can be easily noticeable since the virtual content is supposed to be stable, but now is generally distorted during head turns and induced motion. This study will focus on the perceptual effects caused in this type of distortion, in particular visual disturbance and visual discomfort.

### **1.2 Definition of terms**

1.2.1 Distortion: Distortion refers to angular deviation (x degree, y degree) of simulated virtual content compared to expected location as in real world. There will be distortion when seeing the display through lens in VR headsets, so distortion correction is required to transform the displayed content.

1.2.2 Distortion correction: A process that transform the display image pattern, e.g., make display area into a barrel shape, to achieve a regular and normal virtual world as in real world. It can be done given the optical system of the eye and the location of the eye pupil are determined.

1.2.3 Pupil: The entrance for the light rays to enter the eye.

1.2.4 Dynamic distortion: The changing distortion when users move their eyes, e.g. rotating the head with gaze stabilized, in which the distortion correction is no longer optimal due the changes of the pupil location.

1.2.5 Dynamic distortion correction (DDC): A process that takes in pupil locations in real-time to perform distortion correction.

1.2.6 Distortion map: A 2D vector field representing moving direction and amplitude between two frames of visual inputs, typically used to represent the distortion outcome between two pupil locations. Each vector's pivot represents the initial frame's location, and the vector represents the direction and amplitude of change.

1.2.7 Vestibulo-ocular reflex (VOR): VOR is a reflex that eye gaze is stabilized during head turns, so that the projected image of a physical object remains stabilized on the retina.

1.2.8 Retina: A thin layer of tissue inside the eye at the back to receive light and convert the light into signal sending to the brain.

1.2.9 VOR-type head motion: The head motion that exert VOR, in which the subject is performing head motion with eye gaze stabilized on something, e.g. designed fixation in the virtual scene in experiment.

1.3.0 Subjective Discomfort: The subjective discomfort here refers to physiological responses defined with the continuous discomfort scale used in this study.

### **1.3 Background of the problem**

Compared to that in a physical reality with completely same content, visual input in virtual reality are displayed by screens which are close to eyes. A pair of lenses are required to bend the light and make the image on the retina look like that is observed in a distance. Fresnel lens or hybrid Fresnel lens are wildly used to satisfy the requirements of short focal length and

portability. However, light paths with such a set of optical instruments are different with those in physical environment, so ray tracing methods depending on observation information, e.g. pupil location, can be utilized to apply a parameterized correction to the image. Such correction will change the designated location of image pixels in the VR headset display to cancel out the distortion outcome from lenses.

Nevertheless, a perfect correction requires accurate information about how observer looks through the lens, which is the pupil location relative to the lens. In practice, instead of accurate measurement, an assumption on a fixed pupil location relative to the lens is used, so that the correction for lens distortion is not always perfect and there would be dynamic distortions during the observation with head motion. When a viewer turns head to one side while keeping eye gaze stable with VOR in a VR headset, the pupils move relative to the lens. The assumption on fixed pupil locations relative to the lens is violated and dynamic distortions result from incomplete correction. Thus, during such eye-head movement, light of images from incompletely corrected locations will be bended and projected into pupils, which will introduce dynamic distortion in most, if not all, of the VR headsets in the present time. Having said that, most lenses with built-in correction are good enough to reduce obvious and noticeable distortion near the center region. However, when simulating a virtual world, the peripheral region is also critical that it served to present the virtual environment like floor and ceiling. The twisting image may affect the judgement of reference frame and lead to uncomfortable feelings, such as disorientation and dizziness.

## **1.4 Overview of the study**

### **1.4.1 Experimental work**

The study consists of four experiments: As a preliminary investigation, the studies 1 and 2 were conducted correspondingly for localized distortion conditions and global dynamic distortion conditions, to check whether users are able to perceive dynamic distortion and how severe the discomfort that the conditions would provoke with different distortion levels. To develop a quantitative specification for lens, more controlled experiments were designed and conducted. Participants were asked to subjectively score a set of magnitude-controlled dynamic distortion conditions with controlled head motion, which is referred to as experiment 3. And to validate the

quick rating method, a 20-minute exposure experiment was done, which is referred to as experiment 4.

#### 1.4.2 Predictive model development

To quantify performance of different lens in terms of distortion score and discomfort score, a predictive model was developed and trained with the subjective scores reported for each dynamic distortion condition applied in experiments. The model used ray tracing result with different pupil locations to determine distortion map of each dynamic distortion condition and processed the distortion maps with reference to perceptual effects from literature, then extracted features and used machine learning techniques to estimate the parameters in the model to predict the reported scores in the experiments.

## CHAPTER 2. LITERATURE REVIEW

### Summary

This chapter introduces theories that explain why users may feel discomfort from the visual stimuli experienced in VR headset, and the visual motion sensitivity across the field of view (FOV).

### 2.1 Visually induced motion sickness (VIMS)

Visually induced motion sickness (VIMS) has been discussed a lot as a variant of motion sickness, which is induced by visual experience with limited or absent physical motion. Based on previous studies and literature, there are several theories and hypotheses trying to explain the origin of VIMS. The most widely accepted VIMS theories include sensory rearrangement theory (sensory conflict theory), postural stability theory, oculomotor theory (eye-movement theory) and rest-frame hypothesis.

Postural instability theory hypothesizes pro-long “struggling” to maintain postural stability is at the heart of motion sickness. Inconsistent visual and vestibular stimulus will cause postural instability and symptoms of motion sickness in susceptible subjects (Riccio and Stoffregen, ). The reflex response theory proposed by M.J. Griffin suggest that ocular reflex may play a central role in causing motion sickness and when this theory is combined with the oculomotor theory proposed by S.M. Ebenholtz, one could predict that symptoms of motion sickness may occur among viewers when VR images do not respond correctly to vestibular ocular reflex (VOR) as real images do.

Considering the current context, sensory rearrangement theory and rest-frame hypothesis can provide more direct and relevant explanations on the present questions: whether such visual distortion from dynamic distortion will lead to discomfort like disorientation and dizziness, and how it happens.

Sensory rearrangement theory was firstly proposed by Brand and Reason in 1975 (Bos, 2011; Reason, 1978), which is most widely discussed theory to explain VIMS. It proposes that the mismatch among visual, vestibular and other somatosensory senses will lead to motion sickness symptoms, like what likely happens to an inexperienced observer of a fixed-based flight

simulator, who watching the visual stimulus without adequate vestibular input like that in a real flight experience.

Rest-frame hypothesis suggests the brain has an internal mental model of which objects are stationary (termed as rest-frames) and which are moving. Sensory inputs inappropriate to the brain's motion model, which was considered to make reference selection harder and consume more energy, can cause motion sickness and postural instability (Cao, 2017; Prothero, 1998).

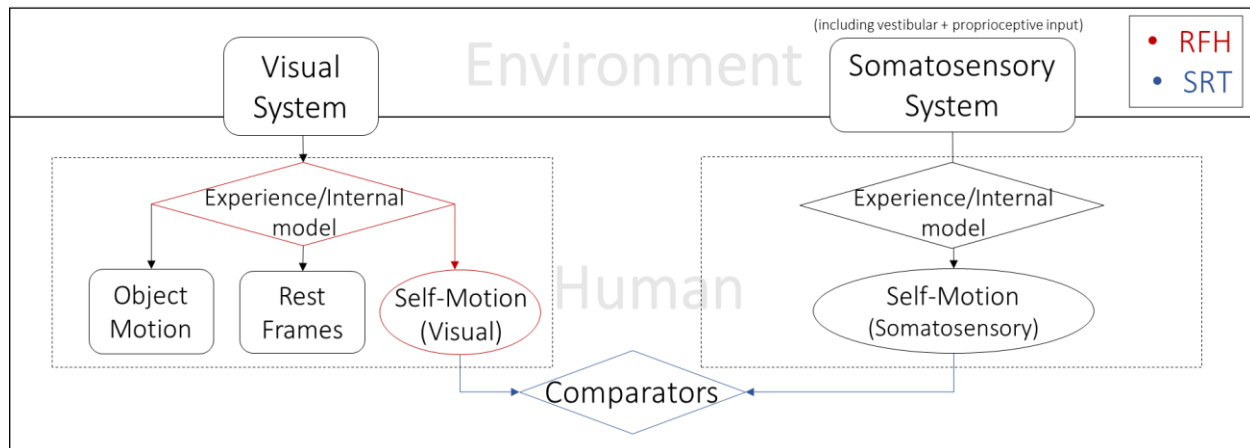


*Figure 1. Two Theories on VIMS: Rest-frame Hypothesis and Sensory Rearrangement Theory: rest frame hypothesis was marked in red: as the internal model from previous experience interpret self-motion, object motion and rest frames from visual input, it may lead to motion sickness if the process was hindered by visual disturbance. Sensory rearrangement theory was marked in blue, where it proposed that the mismatched interpretations of self-motion status from visual and somatosensory system would lead to motion sickness.*

It was acknowledged that the use of computational model to predict subjective discomfort among VR users is not new, previous work have developed cybersickness dose value (CSDV) models to predict levels of nausea among VR users (Chen et al., 2004; Ji et al., 2004, 2007, 2009; So, 1999; Yeun et al., 2002). Although these models are different from the current work because none of them deal with effects of lens distortion, nonetheless, experience from those work assist the current research.

## 2.2 Visual discomfort during VOR

Head movements with vestibular ocular reflex are inevitable in the use of VR systems (So, 1994; So and Chung, 2005; So et al., 1999; So and Griffin, 1995, 2000). In most past studies, the attention have been on the effects of time lags on these head movements on the usability of VR systems. The related studies on effects of lens distortion have received little attention. In this study, subjective visual discomfort was recorded in the watching experience during active horizontal head rotation with a stationary eye gaze. In the real world, the information about self-motion, object motion and rest frame can be inferred from visual cues without disturbance, and that information will align with that inferred by inertial cues from vestibular system. In virtual reality, when viewer doing VOR-type head motion, as pupils are moving relative to lenses, the visual cues may be defective. In the scope of the current study, retinal slips of projected VR images still exist due to head movements. As retinal slips have been shown to affect subjective discomfort among VR users (Guo and So, 2012 and Yang et al., 2011), it is hypothesized that retinal slips due to combinations of head movements and lens distortion will also be noticeable and will cause discomfort among users.

The defective visual cues possibly lead to motion sickness from two aspects. First, the inference of self-motion, object motion and rest frame will be affected as the visual cues are defective compared to that in a real world and they are challenging to our inference model which is based on previous experience. According to rest-frame hypothesis, the defective visual cues will need more effort and resource for inference, which leads to symptoms like motion sickness. Second, the inferred motion and rest frame may not be correct and may conflict with that from inertial cues. After prolonged large exposure and conflict, it will likely lead to motion sickness symptoms, especially to sensitive population.

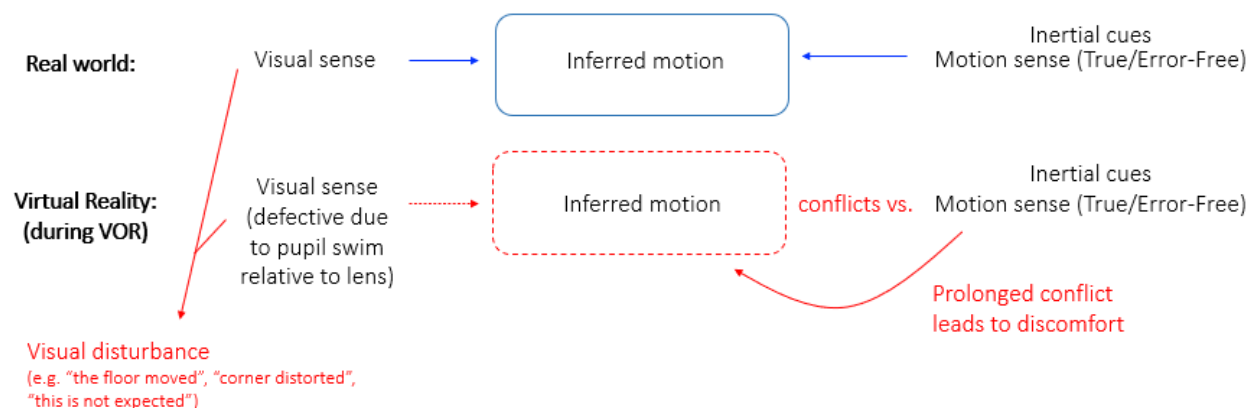




*Figure 2. Hypothetical root cause of motion sickness in VR during VOR-type head motion: As for the cause of motion sickness in current VR scenario, a hypothesis was proposed that, compared to the real world where the sense of motion and rest frame can be normally inferred from visual cues and aligns with that interpreted from inertial cues, in virtual reality, (i) the inference of motion and rest frame would be affected by defective visual cues, so that (ii) the inferred motion might conflict with that from inertial cues. Motion sickness symptoms, like disorientation and vertigo, are likely to be induced after prolonged large conflict.*

### **2.3 Vection and VIMS**

Vection is a self-motion illusion experienced by an individual without real physical self-motion, which is induced by visual motion stimulus in most cases. Many studies on simultaneous vection and VIMS showed that VIMS only happened to those reported vection and vection is likely a prerequisite for VIMS (Smart, 2002; Keshavarz, 2015). Although there are still exceptions where VIMS symptoms may also occur without reporting clear self-motion illusion, the vection-provoking stimulus deserve more attention when it comes to VIMS.

Optical flow was primarily introduced by Gibson as the critical visual cues to determine self-motion status (Gibson, 1950). With the information of the simultaneous optical flow field and focus of expansion (FOE), which is the origin point of all the vectors in the optic flow field, the heading or self-motion can be estimated (Browning and Raudies, 2015). The interpretation of self-motion is vital for the occurrence of visually induced motion sickness, as the theories predicted. In the predictive model in Chapter 4, the self-motion related vector flow in the FOV would be referenced to predict the subjective discomfort score. Unlike the traditional studies of visually induced motion sickness in which vection provoking scene movements were involved (Chen et al., 2011, 2016; Yang et al., 2011), this study uniquely involves only static VR scene.

### **2.4 Visual motion sensitivity across field of view (FOV)**

As the sensitivity to visual motion is not uniform in the FOV, a distortion in peripheral region may not as obvious as one in foveal region to the viewers. It has been recorded with many kinds of visual stimuli that the visual sensitivity decreases with eccentricity and sensitivity along vertical axis are slightly higher than that at a same eccentricity on horizontal axis (McColgin, 1960; Mckee and Nakayama, 1984; Strasburger, 2011). In a study on absolute thresholds in

peripheral vision, the visual sensitivity decreased with eccentricity in an approximately linear relationship and the isogram of visual motion sensitivity was elliptical (McColgin, 1960).

Although the documentation on the sensitivity during VOR-type head motion is not found. A pilot study (pilot study 1) was conducted to test and verify whether the linear relationship and elliptical distribution is also applicable to the visual sensitivity in present case, where viewers are turning head and stabilizing eye gaze with VOR.

## **CHAPTER 3. EXPERIMENTS**

### **Summary**

The study consists of four experiments, pilot study 1 and 2 were conducted for preliminary exploration of the perceptual effects of localized distortion condition and dynamic distortion condition correspondingly. Then experiment 3 was conducted with more controlled design to answer the study question. Finally experiment 4 was conducted to support the validity of the quick rating method in pilot study 2 and experiment 3.

### **3.1 Introduction**

Pilot study 1 investigated the visual motion sensitivity during VOR-type head motion with selected localized distortion conditions. Pilot study 2 was to investigate whether different dynamic distortion conditions would induce differentiable subjective discomforts for a same subject and to test the feasibility of the procedure, where subjects were asked to score each given dynamic distortion condition within a short exposure (a quick rating method) in two aspects: subjective distortion and discomfort.

In experiment 3, subjects were instructed to score a controlled set of dynamic distortion conditions in the same rating method of pilot study 2 and with controlled head motion. In this new set of conditions, the difference among distortion pattern could be compared and analysed with statistical methods. To test the validity of this quick method, experiment 4 was conducted with similar setting as in pilot study 2 and experiment 3 but subjects were now exposed with 20 minutes.

### **3.2 Pilot study 1 - Visual sensitivity during VOR**

#### **3.2.1 Objectives**

Visual sensitivity among view field in stationary observers has been documented by a lot of previous studies, but the visual sensitivity to distortion in FOV during head motion of vestibular ocular reflex is not known for sure yet. The objective of pilot study 1 is to preliminary test the effects with trained testers.

### 3.2.2 Hypothesis

It was hypothesis that the visual sensitivity to distortion can be observed to reduce with eccentricity in an approximately linear relationship when viewers are actively turning head and stabilizing eye gaze with VOR.

### 3.2.3 Method

#### 3.2.3.1 Participants

Two experienced testers participated the pilot study 1, one with normal vision, the other with corrected normal vision.

#### 3.2.3.2 Apparatus and visual scene

The visual content was displayed on XXXXX provided special headset, rendered by Unity 2018 f.3, controlled by an RTX 2080Ti Graphics card and refreshed at 90 Hz. A uniform brick wall scene occupying all visible area during head motion was used as the background. A small white ball was placed in front of the viewer in 2 meters as the fixation point.

#### 3.2.3.3 Visual stimulus

A localized distortion was generated and overlaid on the visual content as the motion stimulus to be observer. The localized distortion will make a localized region in FOV distorted, and the distribution of the distorted magnitude can be described with a 2D-Gaussian function. As for each condition, the localized distortion was not constant but grew with head rotation. During the head turning to the right, the localized distortion appears when head reaches a certain angle, which is referred to as “Onset Angle”; and then it linearly increases to the peak magnitude until the head reached the “Peak Angle”. This growth curve is used to simulate the dynamic distortion which is mild when head orientation aligns with eye gaze and severe when head deviate some degrees from eye gaze. The peak magnitude, which is referred as to the amplitude of a localized distortion, is the major property for a localized distortion condition. The threshold and visual sensitivity are represented with the amplitude.

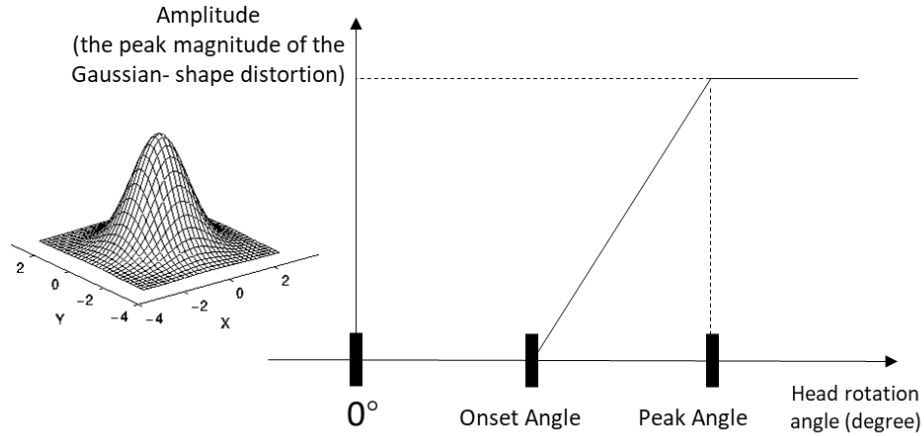


*Figure 3. Localized distortion (2D Gaussian-shape distortion): The localized distortion appeared at a pre-defined eccentricity when head turned 5 degrees to the right (onset angle); the magnitude of localized distortion increased with head rotation and reached the maximum when the head turned to a certain degree (referred to as “peak angle”, i.e. 10, 15, or 20 degrees) to simulate the growth of dynamic distortion. The maximal magnitude was adjusted by the experimenter, referred to as “Amplitude”.*

#### 3.2.3.4 Conditions

The objective of pilot study 1 is to check the visual sensitivity to distortion over the field of view with the eccentricity as the independent variable. Five levels of eccentricity were used, -10, 0, 10, 20, 30 degrees on the horizontal line flush with eye gaze.

The control variables are onset angle, peak angle, the direction of the distortion (upward, leftward and rightward, which is represented by the direction of generation 2D Gaussian-form function) and the size of localized distortion (the area that the localized distortion covers in the field of view, which is represented by the standard deviation  $\sigma$  in the generation Gaussian-form function).

The thirteen sets of conditions used in pilot study 1 are listed below in Appendix 1. For each set of condition, there were five thresholds to be recorded correspondingly at five eccentricities (-10, 0, 10, 20 and 30 degrees). There are 65 localized distortion conditions in total.

### 3.2.3.5 Procedure

After one condition of localized distortion is presented to testers, they were asked to rotate their head actively and naturally from middle to the right while keeping eye gaze on the fixation point. They need to respond “yes” or “no” according to whether the distortion is seen. Level of the stimulus is changed in amplitude from trial to trial using one-down, one-up adaptive procedure. Once the subject report “yes”, stimulus amplitude is decreased by a fixed amount and vice versa.

The run starts with a stimulus (localized distortion) at supra-threshold level and is adjusted with a rather large step size (0.1 degree) until the first no-response. After each reversal point, the step size is decreased to approximately half of the previous one (0.1 decrease to 0.05 then 0.02, 0.01). The run stops when a reverse happen and the difference between 2 adjacent points equals to 0.01. Then the threshold will be the average amplitude of the last two localized distortion conditions.



“+” represents a “yes” response  
“-” represents a “no” response

**Stopping rule:**

The run stops when a reverse happen and the difference between 2 adjacent points equals to 0.01

**Threshold estimation:**

The threshold will be the average of the last two points, for example, 0.105 for the showed figure

*Figure 4. Example of Pilot study 1 Procedure*

### 3.2.4 Results

For one eccentricity, the thresholds recorded in selected 3 standard conditions, which are Left/Right/Up with ramping range 5 to 15 degrees and size 2 with 2 testers, were used to estimate the threshold as shown below in Figure 5. The height of each bar is the mean of thresholds and the length of error bar is the standard deviation at corresponding eccentricity.

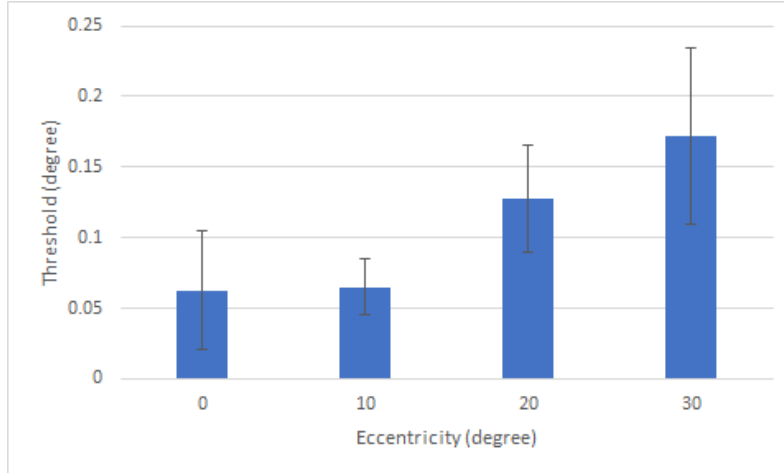


*Figure 5. Thresholds of localized distortions estimated at four sites with different eccentricities (0, 10, 20, 30 degree) on the horizontal line across the gaze point when the head turned to right. The height of each bar is estimated from selected 3 standard conditions (Upward, leftward and rightward and size 2) with 2 testers at different corresponding eccentricity.*

### 3.2.5 Analysis and Discussion

During VOR-type head motion, the thresholds are approximately increasing linearly with eccentricity starting from 10°, which supports the generalization of the linear relationship from stationary observers from literatures and its application in subsequent model. While one difference is that the recorded threshold at the fovea (0°) may be higher than in literature, it may be due to the nature of visual stimulus is different that in this pilot study, subject is observing a patch of smooth distorting pixels. In fact, the Mckee and Nakayama also suggested that the nature of visual stimulus has effect on the threshold and they specifically used different stimulus at the fovea to determine the lowest threshold (Mckee and Nakayama, 1984). However, this pilot study aimed to test the distortion threshold, so a smooth patch of distortion pixels is the only kind of visual stimulus of the study interest. It is worthy to note that, as only 12 combinations of control variables were selected, it is the relative values of averaged thresholds that is informative, instead of absolute values.

### **3.3 Pilot study 2 – Exploration of dynamic distortion**

#### **3.3.1 Objectives**

The dynamic distortions were complained to induce noticeable visual distortion and visual discomfort was also reported after long-term exposure. To verify the visual distortion and discomfort and quantitatively measure those perceptual effects, pilot study 2 collected the subjective opinions from five testers. Similar to Pilot study 1, the objective of Pilot study 2 is to explore different effects with less participants (5 here) and more conditions (75 here). Statistical validations will be conducted in Experiments 3 and 4.

#### **3.3.2 Hypothesis**

It was hypothesized that the dynamic distortion inherited from existing lens design can be observed, and the discomfort scores are related to the distortion level and different lens.

#### **3.3.3 Method**

##### **3.3.3.1 Participants**

Five students at Hong Kong University of Science and Technology were recruited to participate the pilot study. They were well informed and instructed to given subjective scores on dynamic distortion condition during VOR-type head motion.

##### **3.3.3.2 Apparatus and Visual scene**

Pilot study 2 used same equipment in pilot study 1. A visual scene full of buildings was selected from a visual asset called “*Windridge City*”, which is provided by Unity Technologies. A white sphere marked the middle of FOV with a diameter of  $0.025^\circ$ , was acting as the fixation point.

The distance from the observer and the fixation point was eight meters.



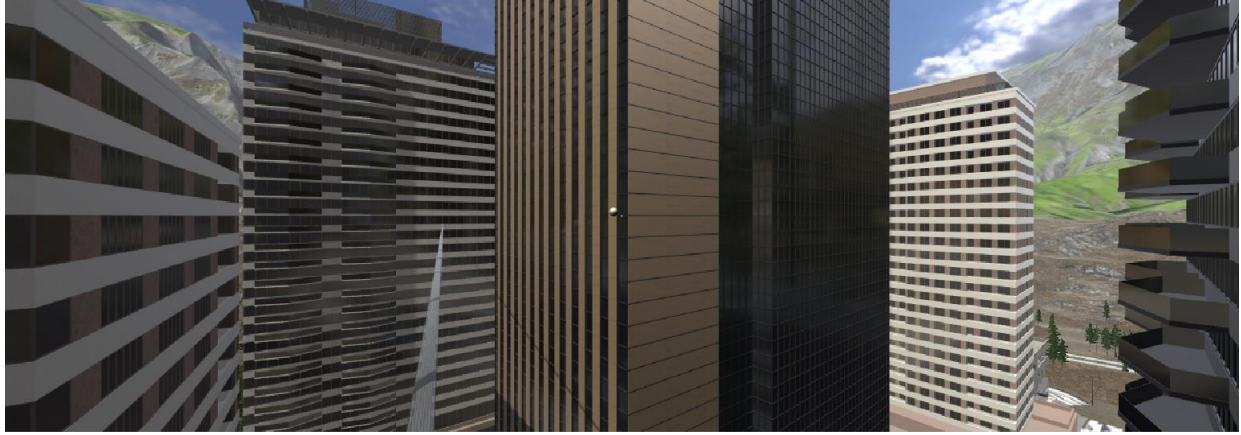


Figure 6. Visual scene used in Pilot study 2 and Experiment 3 and 4

### 3.3.3.3 Conditions

In the pilot study 2, five realistic lens designs were used and corresponding distortion behavior were extracted from ray tracing results., and magnifying or diminishing the distortion effect, 75 dynamic distortion conditions were acquired. To get more insights from limited lenses, 5 modes of variants (numbered as mode 1 to 5, see details in Figure 7) of 5 lenses (total 25 types of distortion map) were generated artificially by selecting different pupil start and stop locations, and adopted as the testing conditions for subjects to rate. For each distortion map, 3 magnification factors were used to adjust the level of distortion: condition with factor “1x” is the original distortion map without magnification; condition with factor “0.5x” halved the vectors magnitude in the distortion map; and condition with factor “2x” doubled the vectors magnitude in the distortion map. In total 75 dynamic distortion conditions ( $5 \text{ lenses} \times 5 \text{ modes} \times 3 \text{ levels}$ ) were designed to be used in pilot study 2.

Lens	Mode	Variants of lens	Level
	#1	original lens distortion	
	#2	lens distortion <b>from 0 to 10°</b> was applied during head rotation from 0 to 10° . After 10° , the distortion stop	
	#3	lens distortion <b>from 10 to 20°</b> was applied during head rotation from 0 to 10° . After 10° , the distortion stop	
	#4	lens distortion <b>from 20 to 30°</b> was applied during head rotation from 0 to 10° . After 10° , the distortion stop	
	#5	lens distortion <b>from 0 to 32°</b> was compressed and applied during head rotation from 0 to 16° . After 16° , the distortion stop	
A	X		0.5x original lens distortion
B			1x original lens distortion
C			2x original lens distortion
D			
E			

Figure 7. Dynamic Distortion Conditions used in Pilot study 2

### 3.3.3.4 Measurement Scale

To get the quantitative perceptual evaluation on dynamic distortion conditions, two subjective scales were used to ask participants to give subjective ratings. The most important question is how much the discomfort that the dynamic distortion condition may lead to after using.

Nevertheless, in the current pilot study, it is not feasible for participant to stay in VR with each condition for a long enough period and report their feelings. And participant after such a potentially VIMS-inducing experience will also need a at least 7-day interval to recover before the next one.

Thus, in the pilot study 2 and following experiment 3, one condition will only be observed for a short time (about 1-2 minutes). And the participants were asked to predict their subjective rating supposing that they were exposed for 20 minutes, with a discomfort scale as shown in figure 8.

The validity of the predictive question will be discussed later in experiment 4.

In this trial, suppose you are exposed in this visual environment for about 20 minutes, how would you assess the scene in terms of discomfort, dizziness and disorientation? Please use a number as response:

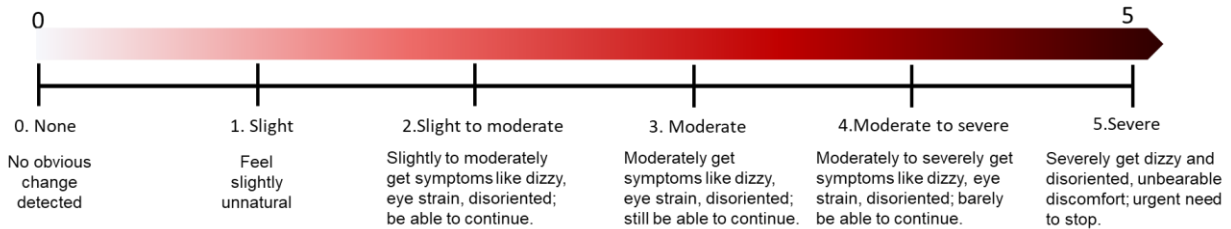


*Figure 8. Discomfort Scale*

To avoid the misunderstanding that the participant might rate for the discomfort with the severity of visual distortion, a question on distortion was asked before the discomfort one, which is the distortion scale as shown in figure 9.

In this trial, comparing with extremely realistic virtual world, how would you assess the scene in terms of image deformation or distortion? Please use a number as response:

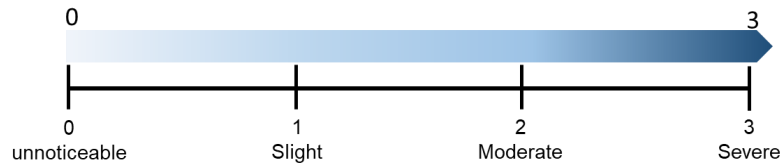


*Figure 9. Distortion Scale*

#### 3.3.3.5 Procedure

Before pilot study, testers were briefed on the procedure and the questions that they were going to be asked. Ten to fifteen conditions were randomly selected to make them be familiarized with the procedure and the range of dynamic distortion conditions. In this pilot study, after a condition was shown, they would keep focusing on the fixation point in the center and rotate head from center to the right with a natural speed and range, which were varied with individuals. With several times VOR-type head rotation and enough observation during the rotation, they were able to score the presented condition with two numbers for two scales. The presentation order was randomized. From the recording of all the pilot studies, subjects could report two scores for a condition after about seven times VOR-type head rotation. After every twelve conditions, they would have a break for five minutes to avoid fatigue and accumulation of discomfort.

#### 3.3.4 Results

The scores from five testers were categorized by lens, mode, and level. The means of discomfort scores are shown in Figure 10. As level increased, the severity of discomfort also increased. As to the type of lens, Lens C and Lens D would lead to higher discomfort scores than Lens A, Lens B and Lens E. Also, different mode of dynamic distortion would lead to ordered preference that mode 5 would lead to higher discomfort score than mode 4, then mode 1, and mode 2 and 3, which are as expected.

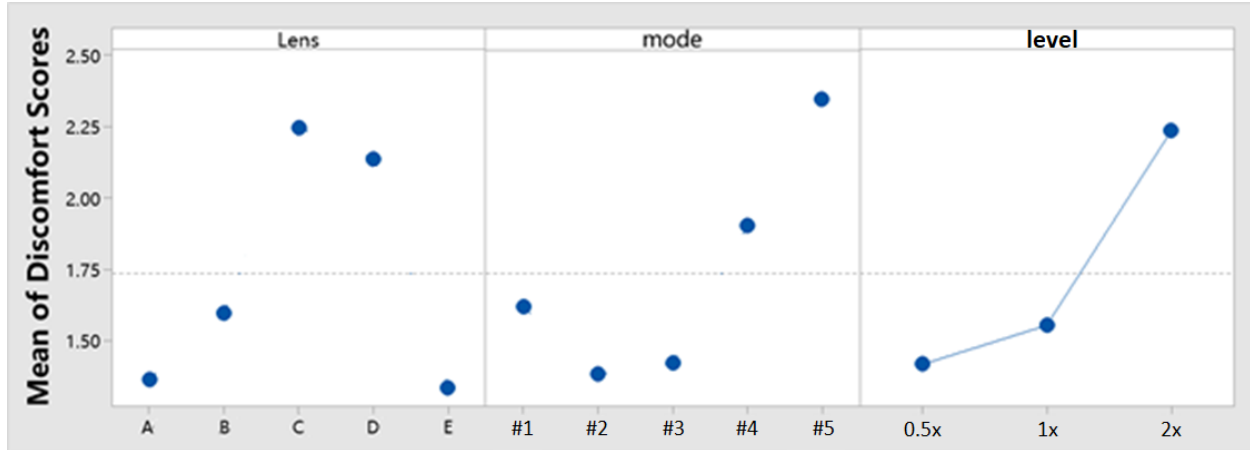
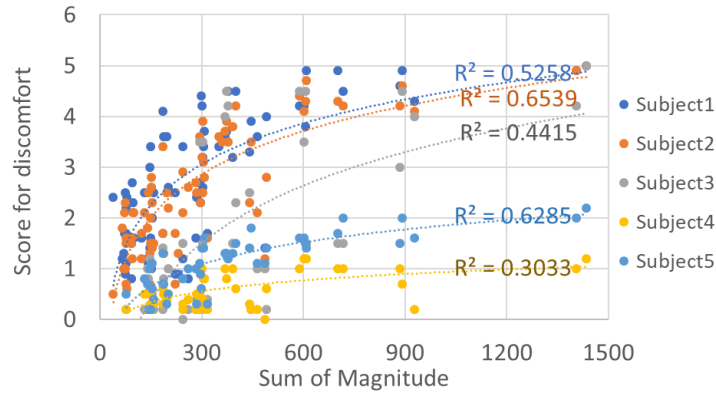


Figure 10. Mean of Discomfort Scores in pilot study 2, demonstrated by types of lens, mode, and level (See detailed definitions in 3.3.3.3): from five subjects in pilot study 2, the severity of discomfort increases with level; on average, according to the discomfort severity of different lens type, Lens C>D>B>A>E, and that of different modes 5>4>1>3>2.

### 3.3.5 Discussion

To investigate the relationship between the intrinsic property of distortion and the discomfort scores, the sum of magnitude of the vectors in distortion map for each condition was calculated. Supposed that the horizontal head rotation was from 0 to 16°, the physical visual distortion exposed to the tester can be extracted from the distortion mapping meshes, which stored the ray tracing results of a set of preset points on the display. A distortion map of this condition under such head motion was defined by extraction from two meshes, one at 0° and the other one at 16°. Sum of magnitude mentioned above was calculated by summing up length of all the vectors in distortion map without consideration of their direction and location in FOV.

The relationship between the discomfort scores and sum of magnitude of each condition was demonstrated in Figure 11A. The discomfort scores of each subject were tentatively fitted with logarithmic functions  $y=a*\ln(x) + b$  and linear functions  $y=a*x + b$ . The coefficients of determination were listed in Figure 11B.



(A)

Fitting Methods	Logarithmic function	Linear function
Subject1	0.5258	0.4939
Subject2	0.6539	0.5829
Subject3	0.4415	0.4429
Subject4	0.3033	0.2716
Subject5	0.6285	0.5625

(B)

Figure 11. The relationship between sum of magnitude and the scores rated for discomfort from five subjects in pilot study 1: (A) five sets of data fitted with logarithmic functions with a form as  $y=a*\ln(x) + b$ . There are 375 data points in Plot (A) representing data from 5 testers x 5 lens conditions x 5 mode conditions x 3 distortion amplitude conditions; (B) the coefficients of determination from logarithmic and linear fitting methods for five subjects are listed in the table.

In general, the relationship between discomfort scores and sum of magnitude are fitted better with logarithmic functions than linear functions, which aligned with the Weber–Fechner law of relationship between actual change in physical stimulus and perceived change. The perceptual effect could be confirmed that the dynamic distortion conditions can induce different levels of discomfort, and a procedure was tested in pilot study 2. Besides, sum of magnitude was found to be a related property of the visual distortion under a dynamic distortion condition.

### 3.4 Experiment 3 – Perceptual effect of dynamic distortion

#### 3.4.1 Objectives

To develop a quantitative model describing the discomfort-provoking ability of a dynamic distortion condition, a good number of observations with diverse and unbiased dynamic distortion conditions are required to acquire numerical labels to train the model. To better control the visual distortion observed under each condition, head motion was controlled in experiment 3. Besides, a full-factorial within-subjects experiment was implemented with a common set of dynamic distortion conditions.

### 3.4.2 Hypothesis

It was hypothesized that both distortion intensity and patterns have significant impact to the discomfort scores.

### 3.4.3 Method

Nine students at Hong Kong University of Science and Technology with normal or corrected to normal vision participated the experiment. The measurement scale and visual scene were identical to those in pilot study 2. Head motion control was implemented to reduce variants in the experiment 3 comparing to pilot study 2. A head motion training and sound cue were provided to guide subjects to perform head motion of range from  $0^\circ$  to about  $16^\circ$  with frequency 0.6 Hz, which were taking reference to pilot study 2 result as a natural move anticipated what would happen as normal users. Power analysis was done based on responses on condition “Lens E, Mode #1, Intensity 100” and “Lens D, Mode #1, Intensity 400”, the Cohen’s d effect size was found to be 1.574. The minimum number of subjects suggested is 7.432 with alpha 0.05 and power of 0.8.

#### 3.4.3.1 Conditions

All 9 subjects rated the same set of lens dynamic distortion conditions. The condition set included combination of four lenses, five modes, and four intensities. Lens C from pilot study 2 was removed since its design is very close to lens D and was an end-of-life product already. The definitions of mode were consistent with those in pilot study 2 (see Figure 7). As for the distortion level, a new definition “Intensity” was introduced by normalizing the sum of magnitude in different conditions to four amounts that were of interest, which are 100, 200, 300 and 400, so that the effect from distortion magnitude and pattern can be better separated. In total 80 conditions were designed.

Lens	X	Mode	Variants of lens	X	Intensity
		#1	original lens distortion		
		#2	lens distortion from 0 to 10° was applied during head rotation from 0 to 10° . After 10° , the distortion stop		
		#3	lens distortion from 10 to 20° was applied during head rotation from 0 to 10° . After 10° , the distortion stop		
		#4	lens distortion from 20 to 30° was applied during head rotation from 0 to 10° . After 10° , the distortion stop		
		#5	lens distortion from 0 to 32° was compressed and applied during head rotation from 0 to 16° . After 16° , the distortion stop		
A					100
B					200
D					300
E					400

Figure 12. Lens-based conditions applied on participants in experiment 3: 8 subjects each were asked to rate 80 conditions (4 lenses \* 5 modes \* 4 intensities) with a controlled head motion.

### 3.4.3.2 Head motion control

Head motion was controlled with a visual feedback training session and a metronome as the audio cue to regulate the head motion frequency. Following the 100-beat-per-minute metronome playing, the subject was trained to actively do horizontal head rotation to the right within the interval between two adjacent beats. When the rotation angle reaches 16° to 20°, a small visual feedback bar on the fixation point will be switch from horizontal orientation into vertical orientation. After 20°, the vertical bar will turn back and keep horizontal. Hearing the beats of metronome, subjects were asked to finish one round-trip head rotation to the range of 16° to 20° every three beats and then come back to the initial position. Figure 13A demonstrates the visual feedback and figure 13B shows the head motion range and speed controlled with the method.

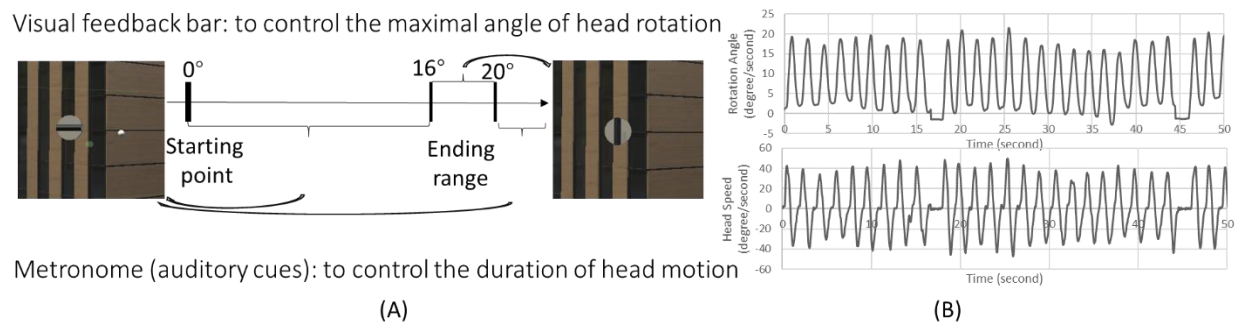


Figure 13. Head motion control and controlled head motion: subjects were trained to rotate head horizontally to the right to a range of 16 to 20° and back to 0°. (A) During the training session before experiment 3, subjects could see a black bar on fixation point and hear a 100-bpm metronome. The bar will turn vertical when the head rotates to a range of 16 to 20° and keep horizontal out of the range. (B) During the experiment, the head motion roughly ranged from 16 to 20° in a uniform frequency.

### 3.4.4 Results

The average discomfort scores by lens, mode and intensity were summarized in Figure 14. The order of four lenses to provoke discomfort were consistent with that in pilot study 2: Lens D>B>A>E. Scores of Lens D was significantly greater than that of Lens E ( $p<0.05$ , Wilcoxon). Discomfort scores for different mode are roughly the same level. The means of discomfort score also increased with the intensity. The effect of intensity was significant ( $p\text{-value} < 0.001$ , Friedman test on average scores for four intensities grouped by eight subjects).



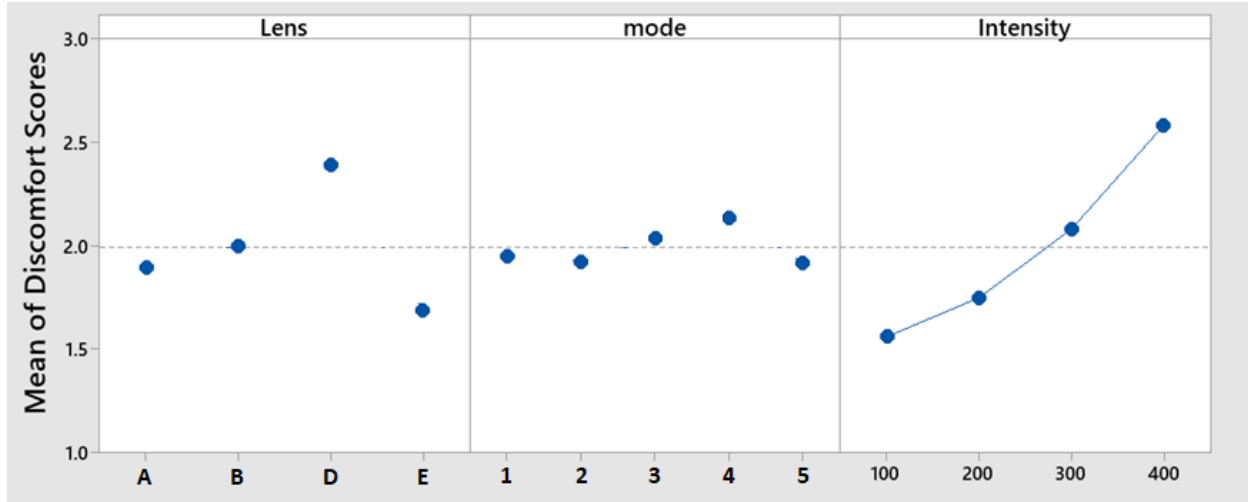


Figure 14. Mean of Discomfort Scores of different lenses, modes and control intensity: data from 80 conditions (4 lenses \* 5 modes \* 4 Intensity) of 8 subjects in experiment 3; means of discomfort among lenses: Lens D>B>A>E, which is consistent with the result of pilot study 2; the severity of discomfort also increased with Sum of Magnitude.

### 3.4.5 Discussion

The discomfort scores increased with the intensity of distortion was expected and significant statistical result was found. While from the first plot in Figure 14, it can be seen that when distortion intensity of conditions was normalized, there were still significant difference between lens design, which means there are intrinsic perceptual effect difference in the distortion maps. This difference could be due to directions of vectors, vectors distribution in terms of location relative to fovea, or consistency of the vector distribution that whether it looks natural and smooth. More details on the analysis would be discussed in Chapter 4 and 5. The order of four lenses after the intensity was controlled,

## 3.5 Experiment 4 – Validation of experiment question

### 3.5.1 Objectives

As considering the limited time and the requirement on a large amount of labelled dynamic distortion conditions, a quick rating method was applied to ask participants to score based on predicted discomfort in 20 minutes in pilot study 2 and experiment 3. To verify whether the scores rated within 2 minutes can predict the subjective discomfort in 20 minutes.

### 3.5.2 Hypothesis

It was hypothesized that the subjective predicted discomfort in pilot study 2 and 3 would be correlated with the actual discomfort score after 20-minute exposure to the same condition.

### 3.5.3 Method

In experiment 4, visual background were the same as those used in experiment 3 and 8 subjects in experiment 3 participated this experiment (one subject dropped out).

#### 3.5.3.1 Conditions

Two conditions of Lens A with a mode #1 were selected as dynamic distortion conditions to be overlaid on the VR environment, one with a magnification factor of 0.5x and the other with 2x, namely A-mode#1-0.5x (abbreviated as A-0.5x) and A-mode#1-2x (abbreviated as A-2x).

#### 3.5.3.2 Task

To keep the participants in the virtual reality environment with the dynamic distortion condition for 20 minutes, two simple head rotation tasks with a fixed eye gaze was introduced and conducted alternatively.

A puppet with a long nose and an antenna was placed at the position of fixation point. The “nose” can be rotated horizontally on the puppet’s face with the head rotation of participants. In the task one, the participants are asked to rotate their head horizontally while focusing on the puppet in the centre, to make the long nose align with the facing direction of the puppet. Except the horizontally rotatable nose, the puppet was fixed at the central position. After 20 times successful nose alignment, one end of the antenna was triggered to swing from left to right with the same frequency of that in experiment 3. The second task was to rotate head from left to right in the frequency while focusing on the puppet for 2 minutes.

#### 3.5.3.3 Procedure

Before the VR exposure, the participant was asked to fill in Simulator Sickness Questionnaire (SSQ) to make sure the baseline status. The VR exposure consists of two alternative tasks will last for 20 minutes. During the 20 minutes, the participant will be asked to report the status with

the discomfort scale every five minutes. After the VR exposure, they were asked to fill in SSQ again to record their symptoms after exposure.

### 3.5.4 Result

#### 3.5.4.1 Quick rating method helps with distinguish the difference between conditions

The scores subjectively predicted before the experiment and during the 20-minute exposure were summarized in Figure 15, with each box consisting of 8 data points at those time stamps. After 20-minute use, scores for A-2x (median = 2.75) were significantly higher than those for A-0.5x (median = 1.85), with a p-value of 0.01403.

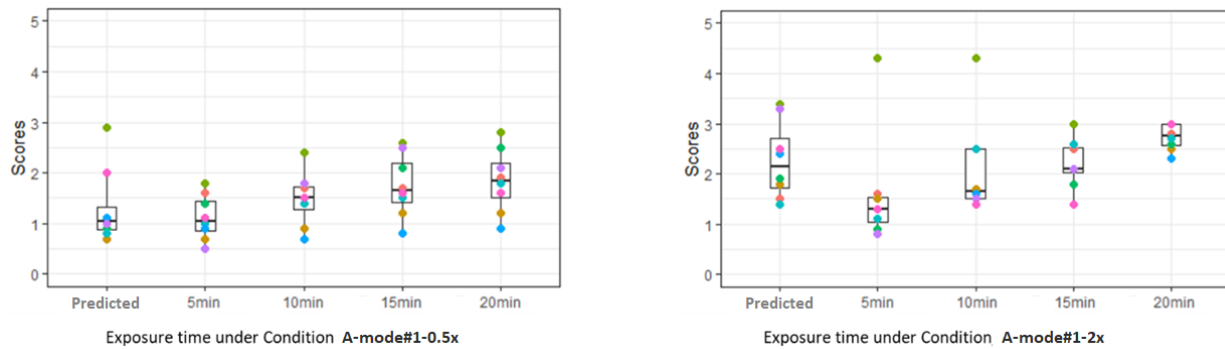


Figure 15. Scores on A-0.5x (Left) and A-2x (Right) before and during 20-minute exposure: the first box contains the discomfort scores reported before experiment, and following boxes are plotted with scores rated by the same 8 subjects every 5 minutes during the 20-minute exposure; points in the same color are from the same subject.

#### 3.5.4.2 Quick rating method recorded the same construct with prolonged experiment 4

The discomfort scores after 20-minute exposure and subjectively predicted before experiment are compared in Figure 15, each point in which are defined with a subjectively predicted scores at the x-axis, and score in experiment 4 after 20-minute at the y-axis.

The connect was drawn between a pair of points determined by scores reported by the same subject, which should be aligned with “y=x” if predicted result with and result from experiment 4 were same outcome. To investigate whether pilot study 2 and experiment 3 were measuring a same construct (discomfort from the dynamic distortion condition) with the 20-minute exposure, the internal consistency indicator Cronbach’s coefficient alpha was calculated based the paired

data, which is 0.7730. As a rule of thumb, Cronbach's  $\alpha > 0.7$  is acceptable, and it is worth noting that Cronbach's  $\alpha$  is thought to underestimate in two-item case. A suggested alternative, Spearman-Brown coefficient was found about 0.8719, and another alternative, standardized Cronbach's alpha was found about 0.7950, which even more supported that the pilot study 2 and experiment 3 were measuring a construct similar to a 20-minute exposure.

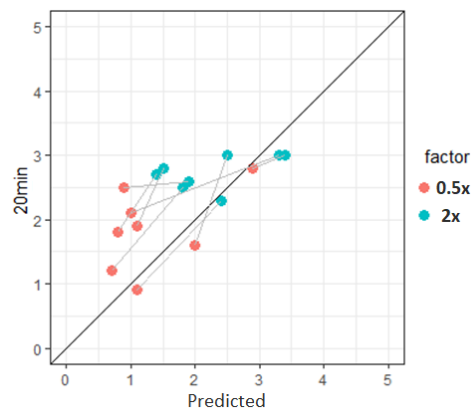


Figure 16. Scores of A-0.5x and A-2x between predicted and after the 20-min exposure: points in red and blue are indicating by discomfort scores for A-0.5x and A-2x conditions, with scores subjectively predicted as x-axis and scores reported after 20-minute exposure as y-axis. The connect was drawn between a pair of points determined by scores reported by the same subject.

### 3.5.5 Discussion

The scoring of discomfort by the quick rating method adopted in pilot study 2 and experiment 3, that subjects were required to predict the discomfort as if they were exposed for 20 minutes, was found to be effective to distinguish the perceptual effect from dynamic distortion between severe and less severe conditions. In fact, even subjects are exposed to the condition after a 5-minute, there was still no significant difference found between scores for two conditions (A-0.5x and A-2x) ( $p > 0.15$  in Wilcoxon signed-rank test). Nevertheless, the subtle difference can be distinguished with the quick rating method in experiment 3, where 8 subjects scored significantly higher for A-2x condition (median = 2.15) than A-0.5x condition (median = 1.05) with a p-value of 0.01415. Based on the paired data, the higher score reported in experiment 3, the higher it would be after 20-minute experiment 4. One other point worth noting is that subjects were, overall, underestimated the discomfort they may experience after 20 minutes, which means the perceptual effect of dynamic distortion is more severe and significant than one may expected.

## **CHAPTER 4. PREDICTIVE MODEL**

### **Summary**

This chapter will describe a predictive model that can be used to takes in the dynamic distortion condition as a distortion map to quantitatively predict the subjective discomfort scores and distortion score that users may give as a figure of merit without the need to fabricate the lens design nor performing user experiment.

### **4.1 Introduction**

Considering the distortion is caused by deviation of pupil location (relative to the lens) from assumption for digital correction, through ray tracing the actual correction at designated pupil locations in the controlled experiment, the distortion can be quantified and represented as 2D fields of arrows (distortion map) overlaying the scene as shown in figure 17. A predictive model was developed and fitted using data from pilot study 2 and experiment 3 to evaluate different patterns and magnitudes of distortion taking reference to realistic lens design.

### **4.2 Model development**

#### **4.2.1 Quantification of dynamic lens distortions**

##### **4.2.1.1 Determination of uncompensated distortion map**

The uncompensated distortion map was defined as the raw distortion vectors in a 2D field for a pair of pupil locations with selected start and end. It is determined by estimating where the pixel content with designated coordinate will show up when the pupil location deviates.

##### **4.2.1.2 Determination of compensated distortion map**

As the content at the fixation point is also distorted during VOR-type head motion, the eyes would track the fixation and the perceived distortion would be different from the raw distortion map. For example, users may not observe any distortion with a distortion map comprised of uniform single direction distortion vectors because the fixation also follows the distortion direction, provided that the magnitude is small enough. Considering the distortion at fovea region, the compensated distortion map is determined by subtracting the distortion at the gaze point to the uncompensated distortion map.

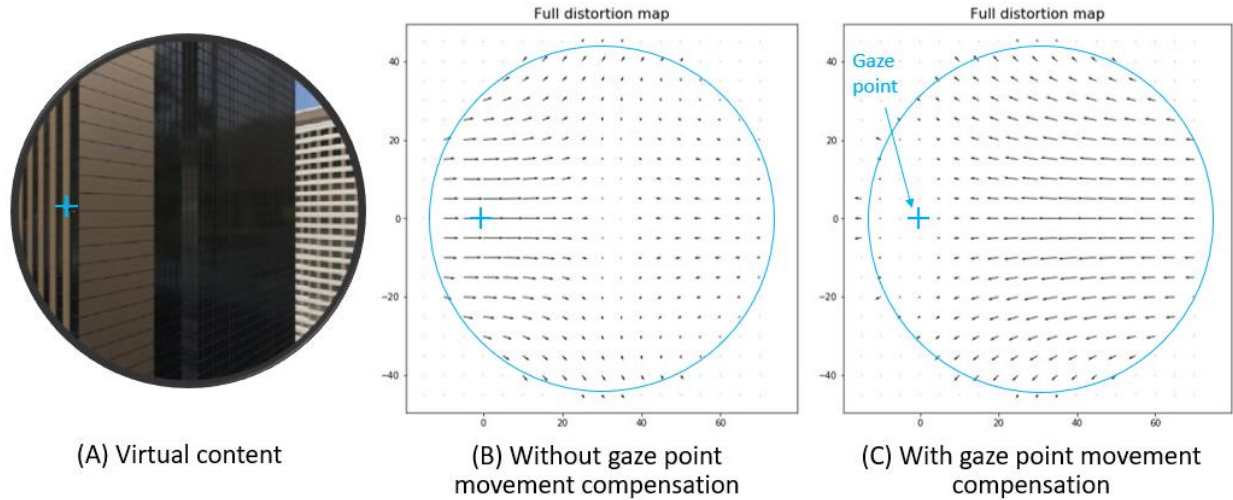
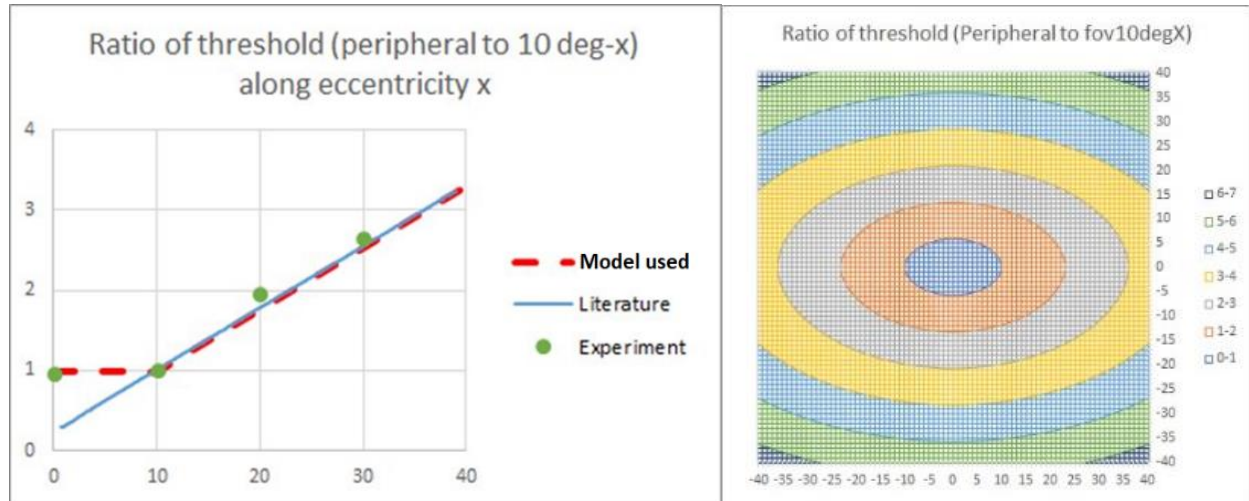


Figure 17. Visual Scene, Uncompensated and Compensated Distortion Map of Certain VOR Head Motion: (A) The visual scene observed at a certain head orientation; The blue cross marked the fixation point and the circle roughly reveal the perceivable field of view. (B) An example of uncompensated distortion map without considering fovea tracking on fixation distortion in the field of view in terms of x and y degrees with reference to fixation. (C) A compensated distortion map based on (B) where the whole map is subtracted by the distortion at the fixation point.

#### 4.2.2 Applying weightings to distortions according to eccentricities

From the literature, it was found that human has a lower sensitivity in terms of motion detection threshold in the peripheral region than the fovea region, and has a ecliptic distribution of motion threshold across FOV (Mckee and Nakayama, 1984). Figure 18A showed the threshold growing linearly along eccentricity, and figure 18B showed the estimated non-linear growing rate across FOV with reference to the literature, where the upper and lower regions have a higher threshold comparing to left and right regions (McColgin, 1960). Pilot study 1 was conducted to verify the literature result with the distortion in VR headset as visual stimulus. As discussed in pilot study 1, there is a deviation in the detection threshold in fovea region ( $0^\circ$ ), which may be due to the nature of stimulus. Therefore, a weighting function inversely proportional to the ratio of threshold relative to  $10^\circ$  position was implemented to the vectors in distortion map in peripheral region, while the weighting within  $10^\circ$  will remain the same as 1. The effect here was expected to be minor to the prediction model, more experiment can be conducted to verify in the future.



(A) Ratio of threshold along eccentricity

(B) Ecliptic distribution of ratio

Figure 18. Justification over the FOV by elliptical weighting function: (A) x-axis represent horizontal eccentricity and y-axis represent ratio of threshold to threshold at  $10^\circ$  eccentricity. Result from pilot study 1 using VR headset (marked by green dots) support the linear relationship between threshold and eccentricity larger or equal to  $10^\circ$ . (B) Referring to the elliptical distribution of threshold on FOV in stationary observer, similar elliptical weighting function was adopted in model in the field of view in terms of x and y degrees, in which different color represent ranges of ratio.

#### 4.2.3 Smoothing to filter out large local distortion vector

Since the distortion size also needed to be large enough especially in the peripheral region as suggested by Mckee and Nakayama (Mckee and Nakayama, 1984), a Gaussian smoothing operation with the filter size increasing with eccentricity is implemented to the distortion map to simulate the global sensation.

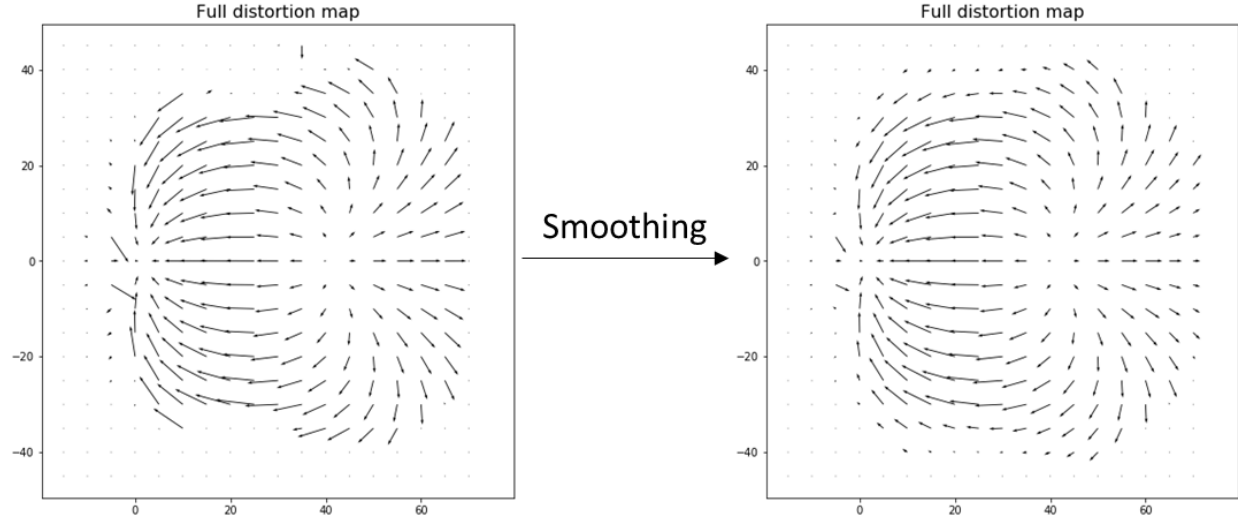


Figure 19. A distortion map before and after smoothing: An example of smoothing a distortion map (left to right), where local distortion in peripheral region is diminished while keeping the overall amount of distortion the same.

#### 4.2.4 Quantifying the spatial-temporal interactions between VOR head movements and the distortions in terms of 6 features

To investigate factors that are potential effective to global sensation, the distortion maps were projected into different distortion patterns inherited from self-motion optic flows, such as forward, backward, yaw, roll pitch rotation. Figure 20 showed the projected distortion map of different patterns from the original distortion map at the middle with blue cross as fixation. The projection was done by applying dot product to the vectors in distortion map with unit vectors depending on patterns. Each of the resulting partial distortion maps will be used as a feature to represent full distortion map for forming the model with machine learning.



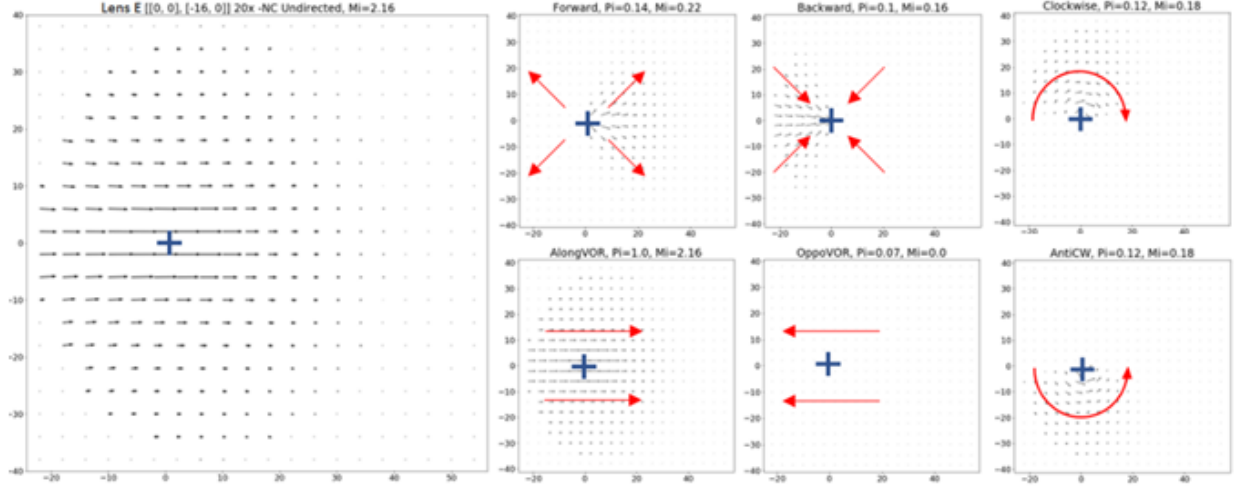


Figure 20. Projecting a visual distortion map: An example of projecting distortion map in different patterns with reference to fixation at the blue cross. The red arrows represent the expected distortion direction of the pattern.

Since the projected distortion maps are only results of dot product, in order to reduce the dimensionality for model training, the distortion map can be consolidated to a scalar similar to sum of magnitude as used in pilot study 2 and experiment 3. However, the sum of magnitude may not accurately represent the quantity of features since both direction and distribution of vectors should agree, so a moderating variable  $p_i$  was introduced to reduce noise where patterns did not match well with its vector direction, the angle differences of the distortion vector relative to corresponding pattern vector were used and summarized into a histogram as shown in figure 21. By fitting the distribution of angle difference with a normal distribution,  $p_i$  was defined by the integrated area within decided range (probability width). Through numerical operation, the probability width was selected at  $80^\circ$  to be stable and near optimal in terms of the mean squared errors in models for distortion and discomfort scores. Note that a normal distribution of the angles was inherently assumed here, the samples do not always follow normal distribution, but the dominant orientation was the main consideration.

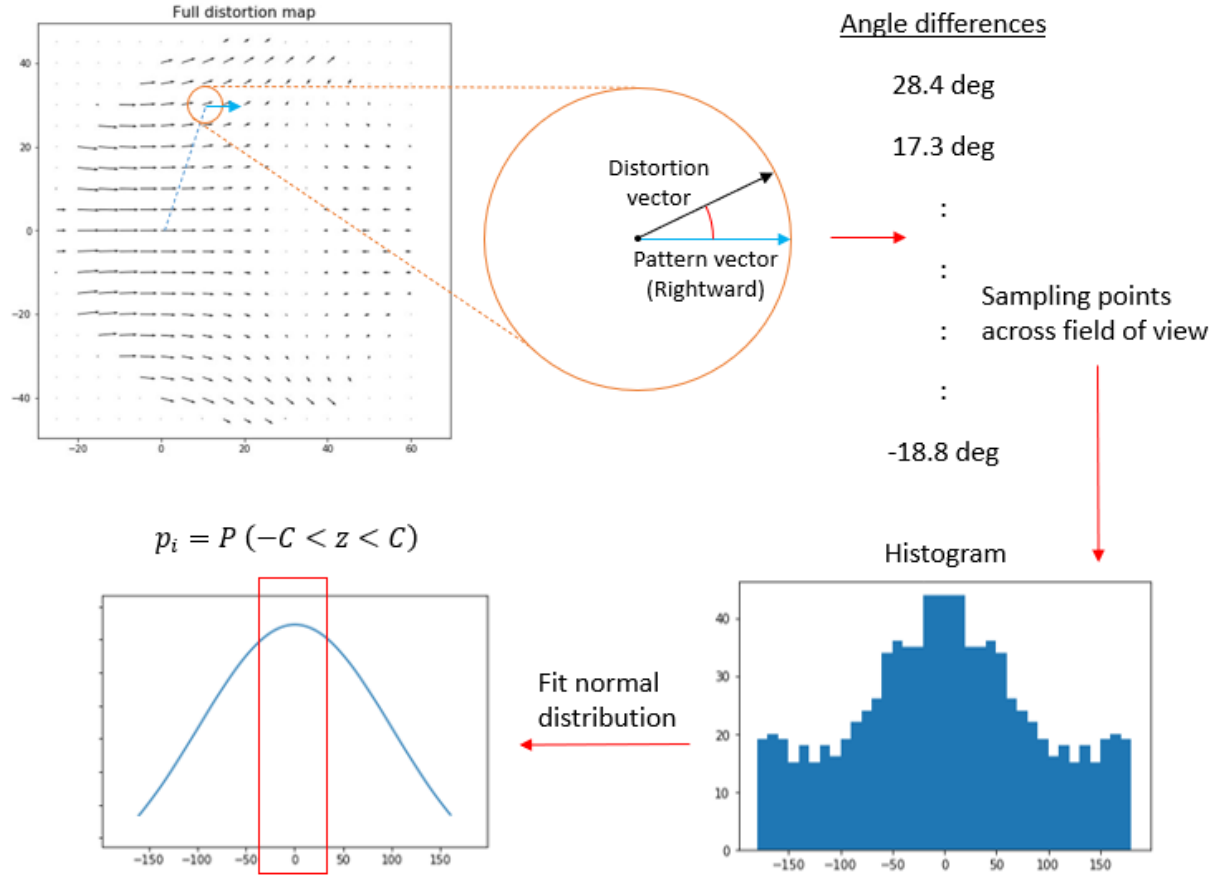


Figure 21. Determination of Probability Width to Filter Valid Distortion Vectors for A Pattern: An example of distortion map, in which a vector is used as illustration of showing angle difference between distortion vector and pattern vector. Histogram of angles differences among all distortion vectors and Along-VOR pattern vector were shown, in which x-axis represent angle difference and y-axis represent frequency. The angle differences were fitted with normal distribution function, that the area under a probability width of  $80^\circ$  ( $\pm 40^\circ$  from center) was used as the moderating variable of that pattern.

To determine features' magnitude, first we have the sum of vectors length in its projected distortion maps:

$$S = \sum_{n=1}^N \|v_n\|, \quad \text{for vector } n = 1, 2, \dots, N \text{ in the distortion map}$$

After determining the moderating variable of feature and sum of vectors magnitude, Fechner's law was applied to the sum of vectors magnitude to represent the perceived strength of stimuli.

The value of sum was added one before the operation since the value itself is relatively small that after logarithm, information was lost if value is below 1. Then, a scale of 0.5 was used to make the perceived level of full distortion map roughly equivalent to the scale of reported subjective score. The  $M$  will then be used as a feature vector to represent the dynamic distortion condition.

$$M_i = p_i[0.5 \ln(S_i + 1)], \quad \text{for component } i = 1, 2, \dots$$

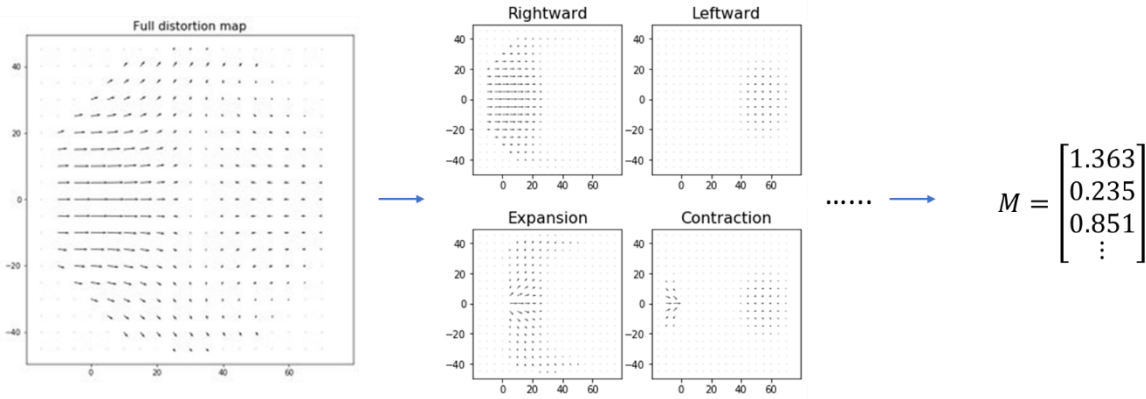


Figure 22. *Determination of features' magnitude:* For each distortion map, after above steps, a list of feature magnitude  $M_i$  will be determined to summarize features' effect to discomfort score and distortion score.

#### 4.2.5 Modeling subjective discomfort as functions of the featured distortion

Lastly, three parameters were introduced to relate the distortion information to the subjective scores, which are  $a_{subj}$ ,  $m_i$ , and a constant.  $a_{subj}$  represents an internal scale used in subject  $j$ , that is related to his/her sensitivity of VIMS, visual acuity or measurement scale;  $m_i$  represent the subjective preference to feature  $i$  that is assumed to be universal to different subjects; and *constant* represent other factors contributing to the score that is controlled or not in scope of study, such as the VOR motion itself and imperfections in simulation that applied to all subjects.

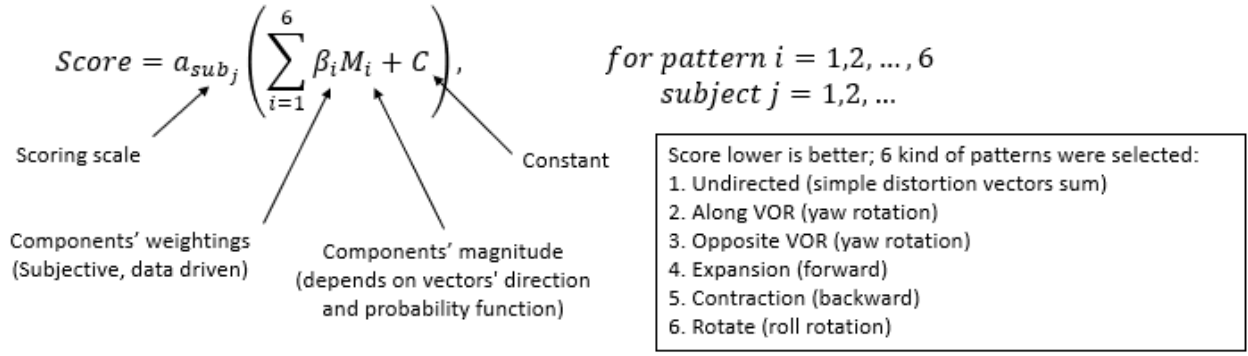


Figure 23. Lens Score Calculation and Selected Features: A brief description of different part of the formula with the 3 new parameters introduced for predicting the discomfort score and distortion score, in which lower is better. To avoid overfitting, maximum value between clockwise and anticlockwise feature was used since the tested distortion conditions were symmetric.

These parameters are estimated through computational optimizer with subject reported data, that the optimizer will minimize mean-squared error between subject reported score and predicted score from the formula, given the  $S_i$  and  $p_i$  obtained from distortion map (stimuli), plus the L2 regularization loss to avoid overfitting to distortion patterns that were experimented.

### 4.3 Model evaluation

Figure 24 showed the subject reported score against predicted score from the model for data collected in the experiment with different distortion patterns or magnitudes. The model generally can predict the reported scores, where desired result is along the line  $y = x$ , while there is a larger variation in prediction result of distortion score, which may be due to the design of model is more inclined to predict discomfort score that global optic flow patterns was mainly considered.

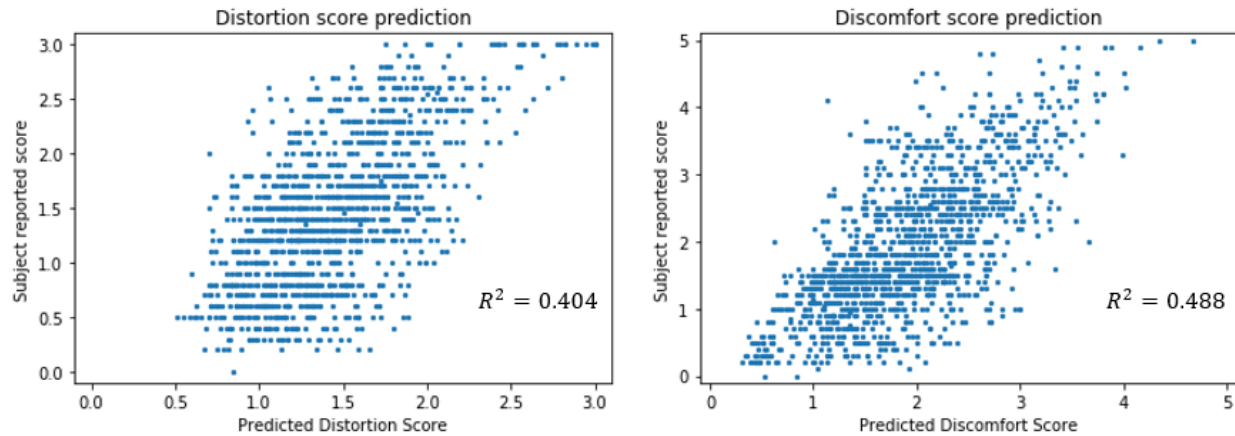


Figure 24. Subject reported score against predicted score from model: X-axis represented the predicted score from model and y-axis represented the reported score the experiment. Left plot showed the prediction result comparison for discomfort score and right plot showed the prediction result comparison for distortion score. A desired outcome should be all dots aligned on the line  $y=x$ .

In order to evaluate the result from experiment and model, native scores of 4 actual lens were plotted to compare the result from experiment and model to prior estimation from XXXXX. The prediction result of intrinsic performance of given lens by comparing the predicted score to the mean of reported score by the subjects in experiment with different modes are also shown in figure 25. The ranking and difference of the lens performance are also revealed by the predictive model similar to reported result, while the absolute scores in some case deviate more, which may be due to limited data available that generated larger variations.

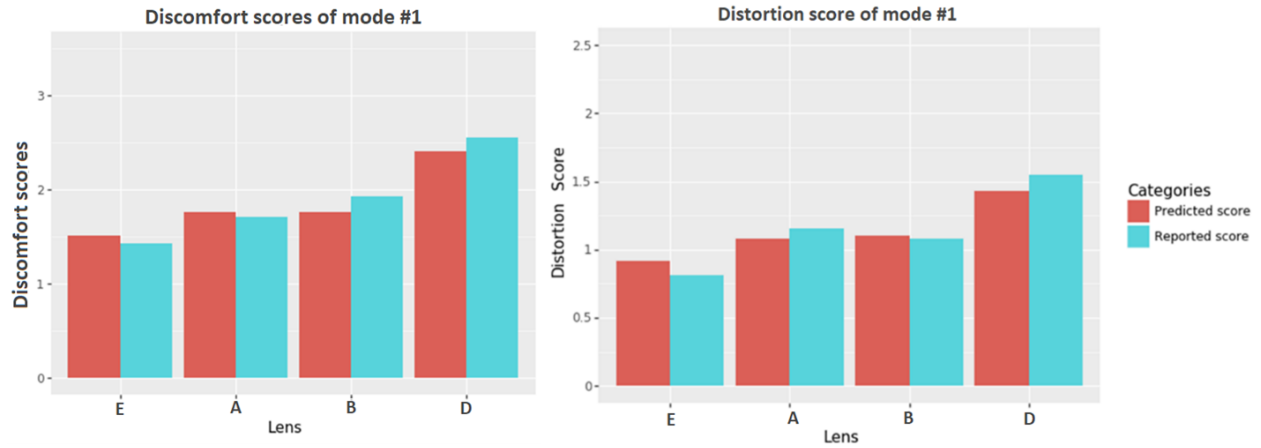


Figure 25. Comparison between Model Prediction and Subject Reported Scores in native lens distortion patterns: The left chart showed comparison between predicted discomfort score and reported score in native lens distortion pattern, and the right chart showed comparison of distortion scores.

## 4.4 Generalizing model

### 4.4.1 Selection of subjective rating scale

Subject rating scale  $a_{subj}$  was involved in the formula, in order to select the right scale for general prediction, a normal distribution was fitted to the subjective rating scales of all subjects in experiment. A scale at different percentile of population can be estimated through the curve to determine a right spec for larger population in evaluating lens. The scale at 90<sup>th</sup> percentile was estimated for general prediction to cover larger population in scoring.

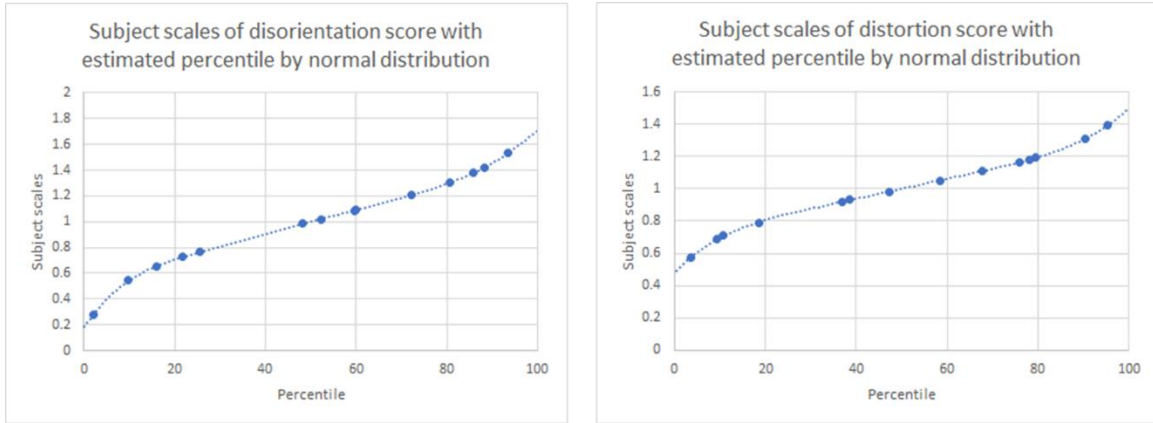


Figure 26. Subjective rating scales and corresponding percentile estimation by normal distribution: Left: scales of discomfort score of 13 subjects; right: scales of distortion score of 13 subjects. The scales of different subjects (y-axis) were estimated in the computational optimizing process and the corresponding percentile of a scale (x-axis) were estimated with the cumulated distribution function of the normal distribution.

#### 4.4.2 Selection of test cases to predict lens score

Since the lens may have varying performance by different pupil start-end locations, a weighted sum approach with different testing conditions, i.e., different pupil location start and end, was adopted to represent the overall score of a lens. Figure 27 showed weighted discomfort score (orange) and distortion score (blue) of different lens with specified weightings. The selection of weightings may change the overall preference of lens, while the effect is generally small comparing 3 types of settings. Note that two untested lenses were introduced here, they were lens designs that were not a product mass produced, while the performance aligns with the

expectation from the company, which also showed the predictability of the model in interpreting new lens design.

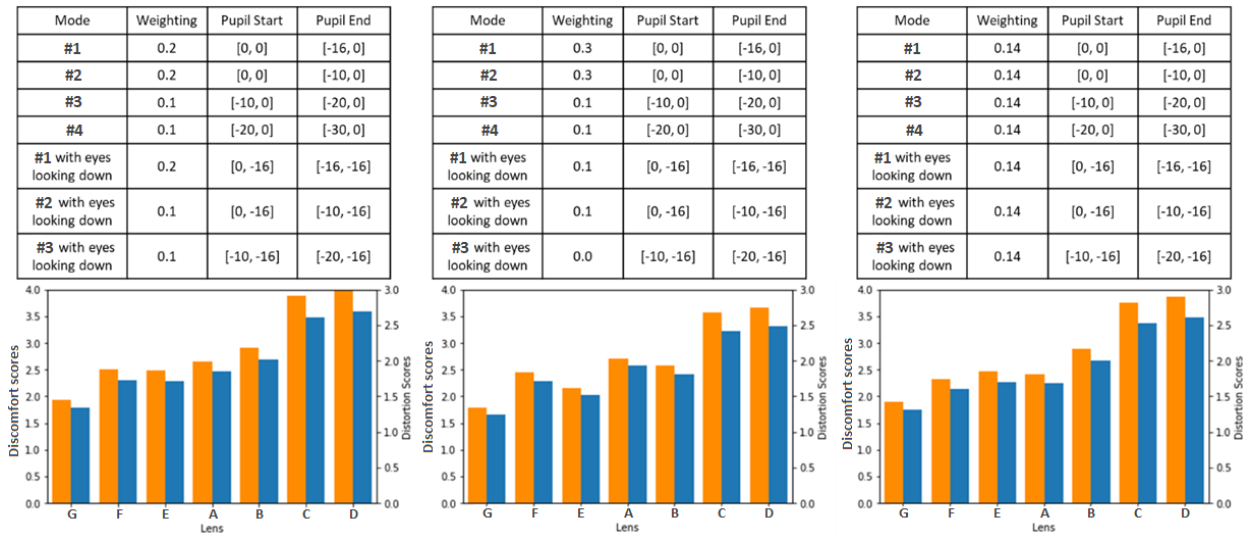


Figure 27. Weighting Selections to comprise an overall lens performance score: There are 7 pairs of pupil start/end locations selected as testing conditions for evaluating the overall score of different lenses, in which pupil start/end is defined as coordinate of the exit pupil in terms of x and y degree with reference to front direction. 3 types of setting were defined and showed in 3 tables, in which weightings are assigned to different testing conditions as shown in the second column. The bottom bar chart in each table represents the weighted sum of scores in each setting for different lens, where the orange bar represented the discomfort score, and the blue bar represented the distortion score.



## CHAPTER 5. DISCUSSION

### 5.1 Lens intrinsic performance

By balancing the conditions rated by all the subjects, dynamic distortion conditions can be compared with equal number of subjective ratings. Those discomfort scores under original lens dynamic distortion conditions (mode #1 and level 1x), instead of a variant or a magnified lens dynamic distortion condition, are more directly related to the intrinsic performance of lenses. In Figure 28, the scores are summarized and compared between each pair of lenses. Each box represented scores from 8 subjects in experiment 3.

The rankings of the original lens conditions are consistent with the conclusions from average discomfort scores including all variants and magnified conditions originating from original lens dynamic distortion conditions, which is that Lens D would come with discomfort scores significantly higher than all the other lenses, Lens E would be with lowest discomfort scores, and that Lens A and B were in the middle without significant difference between them (Wilcoxon signed-ranking test, p-values were labelled in the Figure 28).

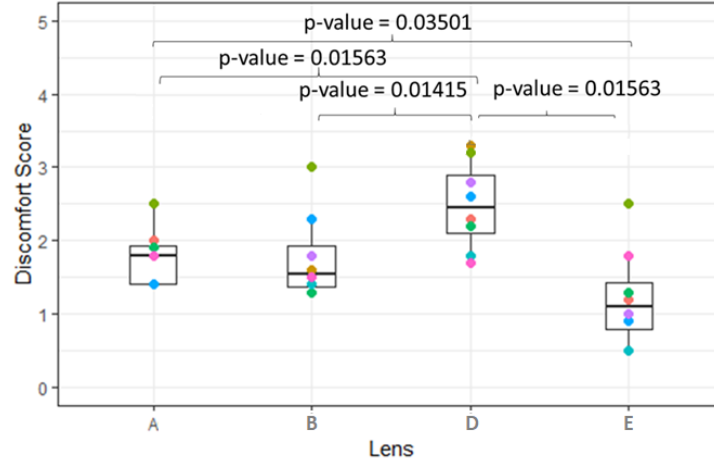


Figure 28. Discomfort evaluation on lens intrinsic conditions: data from discomfort scores of 8 subjects in experiment on lens intrinsic conditions, which are dynamic distortion conditions with mode #1 and a level of 1x. Each box is corresponding to one lens, with black horizontal lines denoting the medians of discomfort scores. P-values are from Wilcoxon signed-rank test between scores of two lens in which those smaller than 0.05. Overall, the ranking to induce discomfort with significance is Lens D>A>E and Lens B should be somewhere between Lens A and E.

## 5.2 SSQ symptoms corresponding to discomfort score

The correspondence between SSQ symptoms and three subscales, “Nausea”, “Oculomotor” and “Disorientation”, were shown in Figure 30A. Subjects in experiment 4 were asked whether they got any SSQ symptoms (Figure 30A) after 20-min exposure to two dynamic distortion conditions (A-0.5x and A-2x). Looking into the SSQ symptoms reported by subjects for two conditions (Figure 30B), it was found that those symptoms subject to the “Oculomotor” subscale were reported more (see Figure 30C).

Symptoms reported after 20-minute exposures to condition A-0.5x and A-2x were shown in Figure 30B in light blue and dark blue, correspondingly. As from the subjective ratings, A-2x induced higher scores in discomfort scale than A-0.5x condition, the SSQ symptom reported more frequently in A-2x than that in A-0.5x was considered to be more relevant to the discomfort scale and the perceptual effects of dynamic distortion, which include “vertigo”, “fullness of head” and “general discomfort”.

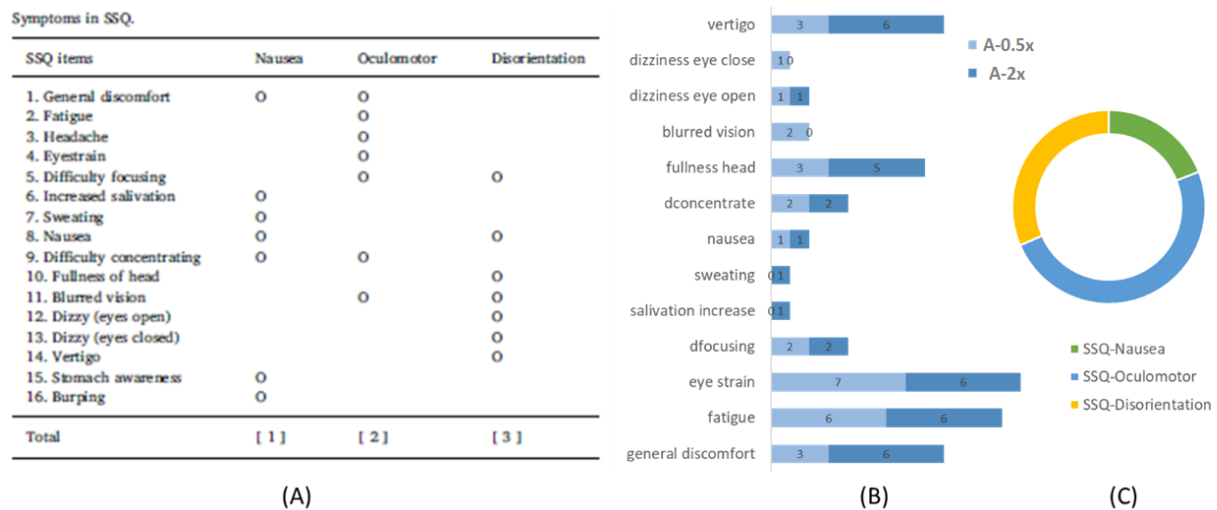


Figure 29. SSQ symptoms reported after 20-min exposure to two dynamic distortion conditions (A-0.5x and A-2x): (A) the correspondence between SSQ symptoms and three subscales; (B) the frequency of SSQ symptoms reported for two dynamic distortion conditions, where darker bars show the frequency for A-2x condition and lighter bar shows that for A-0.5x condition. It was found that 1-general discomfort, 10-fullness of head and 14-vertigo were more frequently

reported in A-2x than A-0.5x. (C) The number of symptoms reported in both conditions was counted by three subscales of SSQ: nausea, oculomotor, and disorientation.

### 5.3 Prediction on new lenses or cases with fixation not on x-axis (head tilting)

The predicted scores when fixation not on x-axis is higher as expected as shown in figure 32, since it is more near to the edge of lenses. While some lenses are less affected such as Lens F, which is preferable and can be reflected in weighted scores. The effect in scores was revealed through distortion map comparison between Lens F and Lens E in figure 32. There is roughly similar amount of distortion in Lens F even head tilted, while the distortion is comparatively severe in Lens E.

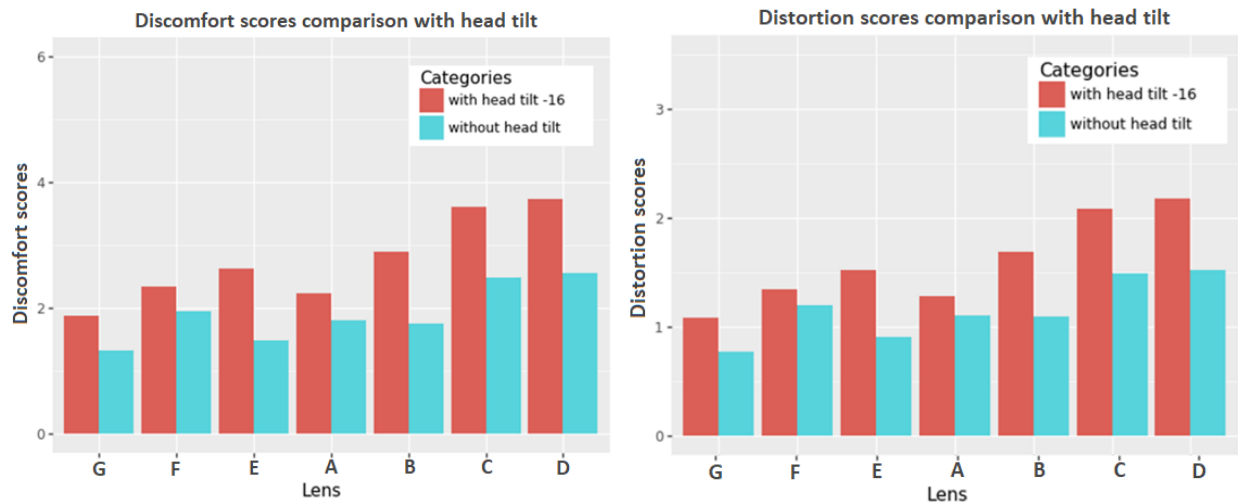


Figure 30. Predicted distortion scores for lenses with fixation not on x-axis (head tilt): The above charts showed comparison of same VOR-type head motion with or without fixation offset from x-axis in field of view in different testing conditions. The scores with offset are predicted generally higher in all testing conditions. The left chart showed comparison of discomfort score and the right chart showed comparison of distortion score.

### 5.4 Estimating the scale at 90<sup>th</sup> percentile of population for discomfort score

Figure 33 showed two ways to estimate the scale for 90<sup>th</sup> percentile of population, one is assuming the scales for population is normally distributed, and the subjects represented the population that the scale for 90<sup>th</sup> percentile would be  $\text{mean} + 1.28 * \text{sigma}$ ; the other one takes in the MSSQ score of each subject to represent their percentile in population and perform linear

regression to estimate the scale. Since there is not strong support on the correlation between subject scale and MSSQ score, the former approach is adopted.

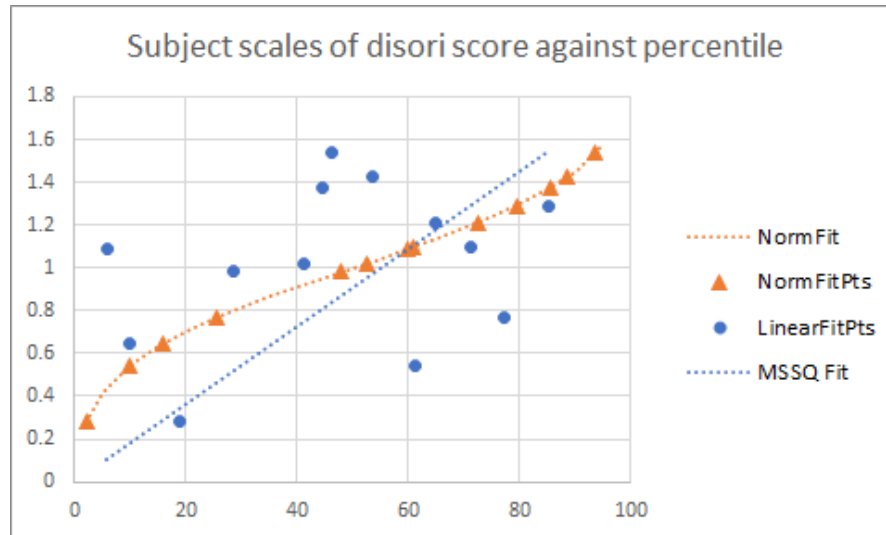


Figure 31. Comparison between Subject Scale and Motion Sickness Susceptibility Questionnaire (MSSQ) Scores: Y-axis represent the subject scales estimated from computational optimizer and x-axis represent the percentile of population. The blue data points showed the approach of using the MSSQ score to represent the percentile of population for finding the scale at different percentiles, and the orange data points used estimated percentile from estimated normal distribution curve.

## **CHAPTER 6. CONCLUSIONS, LIMITATIONS AND FUTURE WORKS**

### **6.1 Conclusions**

The current study investigated and modelled the perceptual effect associated with dynamic image distortion during a VR experience resulted from imperfection of lens. Specifically, the perceptual effects included distortion noticeability, discomfort and all the other possible motion-sickness related symptoms.

Data indicate that the design of lens can significantly affect the levels of discomfort and the levels of discomfort increases with increasing distortion intensity. In particular, the intrinsic performance of lenses can significantly affect the discomfort ratings. Empirical data show that participants can accurately predict visual discomfort ratings associated with a hypothetical 20-minute exposure even though they are only exposed for 1 minute or less. Analysis of the discomfort ratings and data collected from the commonly used Simulator Sickness Questionnaires (SSQ) suggest that the discomfort caused by the dynamic distortion are related to symptoms of vertigo, fullness of head and general discomfort.

A data-driven figure of merit (FOM) predictive model has been reported (Chapter 4). With the distortion map as the quantitative representations of dynamic distortion of a particular lens, the FOM model can predict the associated discomfort ratings to be experienced by users exercising head motions in VR simulations. The model has been shown to be able to rank the lens design according their predicted visual discomfort and the ranking are consistent with the expected quality of the lens design provided by the industry and is being used by the sponsored company in the quality control process in manufacturing plant.

The FOM model demonstrated to successfully predict the perceptual discomfort associated with the lenses and cases with head tilting down. The model can also be tuned to estimate the discomfort scores for selected percentile (e.g., the 90<sup>th</sup> percentile) of user population. Fitted parameters of the FOM model indicates that the modeled dynamic distortion in the form of distortion map should be interpreted according to directional patterns rather than direct summation of distortion vectors.

In summary, this study demonstrated an approach to evaluating the quality of VR displays from the two aspects of user study and data-driven method. With the definition of discomfort scale, the specification can be defined for tolerance of lenses performance in VR experience.

## **6.2 Limitations and future works**

### **6.2.1 Limitation**

In the present work, only the conditions with head rotation to the right from 16 to 20 degrees and mainly four lens designs had been tested in the experiments. The scope of this work focuses on perceptual difference among lens designs, so only one VR scene and head motion setting was tested, i.e. horizontal-direction VOR head movement between 0 and 16 degrees. Different VOR head motion setting can be tested, for example, horizontal-direction VOR head movement with head tilt and vertical-direction VOR head movement.

### **6.2.2 Future work**

Following the study on various dynamic distortion conditions with controlled head motions, data associated with more diverse distortion conditions, head motion modes and more participants are desirable. In the discussion, a prediction on conditions with head tilting down was provided, while the head tilt case was not experimented, in which the distortion pattern was a bit different than the one tested in terms of Upward and Downward patterns, the prediction result may need to be validated in future empirical studies.

## **Bibliography and References**

- Bos, J. E., (2011) Nuancing the relationship between motion sickness and postural stability, *Displays*, vol. 32, no. 4, pp. 189–193.
- Browning, N. A. and Raudies, F., (2015) Chapter 18 : Visual Navigation in a Cluttered World.
- Cao, Z., (2017) The effect of rest frames on simulator sickness reduction, no. July 2017.
- Chen, D., Bao B., Zhao Y., So, R.H.Y. (2016) Visually induced motion sickness when viewing visual oscillations of different frequencies along the fore-and-aft axis: Keeping velocity constant versus amplitude constant. *Ergonomics*, 59(4), 582-590.
- Chen, R., Ho, A., Lor, F. and So, R. (2004) Enhancing the predictive power of cybersickness dose value (CSDV) to include effects of field-of-view and binocular views. *Proceedings of the 7th International Conference on Working With Computing Systems 2004*, 29 June ?2 July, Kuala Lumpur, Malaysia.
- Chen, W., Chen, J.Z and So, R.H.Y. (2011) Visually induced motion sickness: effects of translational visual motion along different axes. *Contemporary Ergonomics 2011* (Eds: Paul T. McCabe), Taylor & Francis.
- Gibson, J. J., (1950) *The perception of the visual world*. Oxford, England: Houghton Mifflin.
- Guo, C.T., So R.H.Y. (2012) Effects of foveal retinal slip on visually induced motion sickness: a pilot study. *Proceedings of the 56th Annual Meeting of the Human Factors and Ergonomics Society*, Oct., Boston, MA, USA, pp. 2560-2569.
- Ji, J.T.T., So, R.H.Y. and Cheung, R. (2009) A bi-computational model to predict visually induced nausea levels in the presence of vection. *Proceedings of the 2nd International Symposium of Visual Image Safety*, Utrecht, Netherlands (VIMS2009).
- Ji, J.T.T., Lor, F.W.K. and So, R.H.Y. (2004) Integrating a computational model of optical flow into the cybersickness dose value prediction model. *Proceedings of the 48th annual meeting of the Human Factors and Ergonomics Society*, 20-24 September, New Orleans, LA, USA.
- Ji, J., Chow, E., Lor, F., So, R.H.Y., Cheung, R., Stanney, K. and Howarth, P.A. (2007) A biologically inspired computational model relating vection and visually induced motion sickness:

individual effects and sensitivity analyses. Proceedings of the First International Symposium on Visually Induced Motion Sickness, Fatigue, and Photosensitive Epileptic Seizures (VIMS2007), 10-12 Dec., Hong Kong. pp.33-40.

Keshavarz, B., Riecke, B. E., Hettinger, L. J., and Campos, J. L., (2015) Vection and visually induced motion sickness: how are they related?, *Front. Psychol.*, vol. 6, p. 472

McColgin, F. H., (1960) Movement Thresholds in Peripheral Vision, *J. Opt. Soc. Am.*, vol. 50, no. 8, p. 774.

McKee, S. P. and Nakayama, K., (1984) The Detection of Motion in the Peripheral Visual Field, *Vision Res.*, vol. 24, no. 1, pp. 25–32.

Prothero, J. D., (1998) The Role of Rest Frames in Vection, Presence and Motion,

Reason, J. T., (1978) Motion sickness adaptation: a neural mismatch model., *J. R. Soc. Med.*, vol. 71, no. 11, pp. 819–29, Nov.

Riccio, G. E. and Stoffregen, T. A., (1991) An Ecological Theory of Motion Sickness and Postural Instability, *Ecol. Psychol.*, vol. 3, no. 3, pp. 195–240.

Smart, L. J., Stoffregen, T. A., and Bardy, B. G., (2002) Visually induced motion sickness predicted by postural instability, *Hum. Factors*, vol. 44, no. 3, pp. 451–465

So, R.H.Y. (1994) An investigation of the effects of lags on motion sickness with a head-coupled visual display. U.K. Informal Group Meeting on Human Response to Vibration, Institute of Naval Medicine, Alverstoke, Gosport, England, September 19-21, 1994.

So, R.H.Y., (1999) The search for a Cybersickness Dose Value. Proceedings of the 8th International Conference on Human-Computer Interaction. August 22-27, 1999, Munich, Germany.

So, R.H.Y., Cheung, K.M. and Goonetilleke, R.S. (1999) Target-directed head movements in a head-coupled virtual environment: predicting the effects of lags using Fitts' law. *Human Factors*, Vol.41, No.3, 1999, pp. 474-486.

So, R.H.Y. and Chung, G.K.M. (2005) Sensory motor responses in virtual environments: predicting the effect of lags for target-directed hand movement. Proceedings of the 27th annual



international conference of the IEEE Engineering in Medicine and Biology Society, 1-4, September, Shanghai, PRC.

So, R.H.Y., Finney, C.M. and Goonetilleke, R.S. (1999) Motion sickness susceptibility and occurrence in Hong Kong Chinese. *Contemporary Ergonomics 1999*, Taylor & Francis, pp.88-92.

So, R.H.Y. and Griffin, M.J. (1995) Head-coupled virtual environment with display lag. Chapter 5 in: *Simulated and virtual realities*, Editors: K.Carr and R. England. Published: Taylor and Francis, London, 1995

So, R.H.Y. and Griffin, M.J. (2000) Effects of target movement direction cue on head-tracking performance. *Ergonomics*, Vol.43, No.3, pp. 360-376.

Strasburger, H., (2011) Peripheral vision and pattern recognition: A review, *J. Vis.*, vol. 11, pp. 1–82.

Yang, J.X., Guo, C.T., So, R.H.Y. and Cheung, R.T.F. (2011) Effects of Eye Fixation on visually induced motion sickness: are they caused by changes in retinal slip velocity? *Proceedings of the 55th annual meeting of the Human Factors and ergonomics Society*, 19-24 September, Las Vegas, USA.

Yuen, S.L., Chen, R.W. and So, R.H.Y. (2002) A progress report on the quest for a cybersickness dose value. *Proc. of 46th HFES Annual Meeting*, Baltimore, MD, pp.2189-2192.

### Appendix A. Set of localized distortion conditions in pilot study 1

Onset Angle (degree)	Peak Angle (degree)	Size (degree)	Direction	Tester	Eccentricity (degree)
5	15	2	Up	1	{-10, 0, 10, 20, 30}
5	15	2	Right	1	{-10, 0, 10, 20, 30}
5	15	2	Left	1	{-10, 0, 10, 20, 30}
5	15	4	Left	1	{-10, 0, 10, 20, 30}
5	15	6	Left	1	{-10, 0, 10, 20, 30}
5	15	8	Left	1	{-10, 0, 10, 20, 30}
5	15	2	Right	2	{-10, 0, 10, 20, 30}
5	10	2	Left	2	{-10, 0, 10, 20, 30}
5	15	2	Left	2	{-10, 0, 10, 20, 30}
5	20	2	Left	2	{-10, 0, 10, 20, 30}
5	15	2	Up	2	{-10, 0, 10, 20, 30}
5	20	2	Up	2	{-10, 0, 10, 20, 30}
5	20	4	Up	2	{-10, 0, 10, 20, 30}

## Appendix B. Observations on testing conditions in pilot study 2 and experiments 3 & 4

Subject	Head Motion	Conditions
#1	Natural motion without external control	75 conditions = 5lenses $\times$ 5modes $\times$ (0.5x, 1x, 2x)
#2		
#3	Controlled with a slower speed	58 conditions = 5 lenses $\times$ 5 modes $\times$ (0.5x, 2x) + 8 $\times$ (0.5x)
#4	Controlled motion	61 conditions = 5 lenses $\times$ 5 modes $\times$ (0.5x, 2x) + 11 $\times$ (0.5x)
#5		58 conditions = 5 lenses $\times$ 5 modes $\times$ (0.5x, 2x) + 8 $\times$ (0.5x)
#6		50 conditions = 5 lenses $\times$ 5 modes $\times$ (200, 400)
#7		45 conditions = 5 lenses $\times$ 3 modes $\times$ (0.5x, 2x) + 15 $\times$ (0.5x)
#8	Controlled motion	92 conditions = 4 lenses $\times$ 5 modes $\times$ (100,200,300,400) + 4 lenses $\times$ (mode#1) $\times$ (0.5x, 1x, 2x)
#9		
#10		
#11		
#12		
#13		
#14		
#15		
#16	Controlled motion	80 conditions = 4 lenses $\times$ 5 modes $\times$ (100,200,300,400)